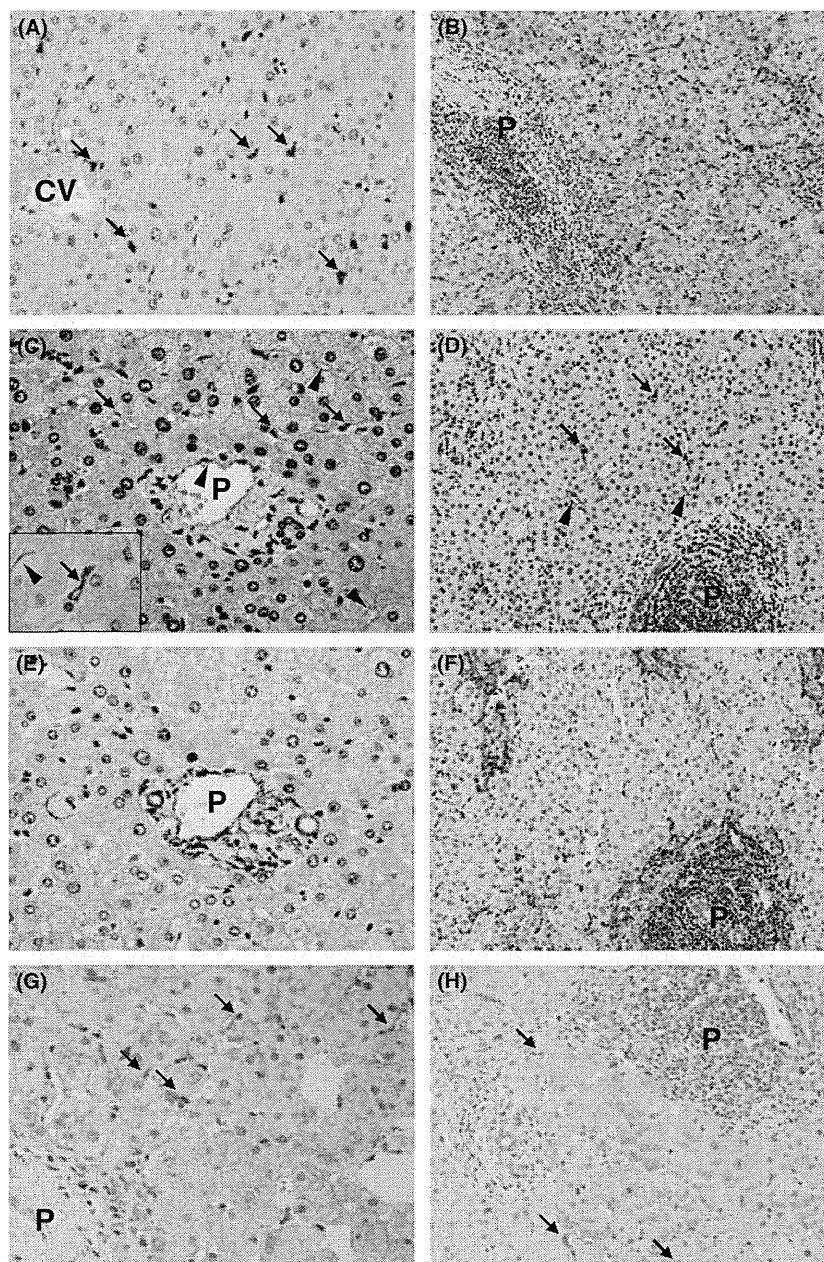


inobenzidine tetrahydrochloride (DAB; Dojinkagaku, Japan) and 0.1% hydrogen peroxide in 50 mM Tris buffer (pH 7.6) at room temperature. The sections were lightly washed, counterstained with haematoxylin, dehydrated in ethanol and mounted with Permount.

For double immunostaining of LRAT/SMA, LRAT/CD31 and LRAT/CRBP-1, a Ventana XT System

Benchmark (Ventana Medical Systems, Inc., Tucson, AZ, USA) (automated immunohistochemical instrument) was used. Double immunostaining was performed using antibodies at the same dilutions as described above except for CD31 (1:20). The immunoreaction was visualized by using an i-View DAB and RED detection kit (Ventana Medical Systems, Inc.) for each antibody.



**Fig. 2.** Immunostaining of normal METAVIR score F0A0 (A, C, E, G) and fibrotic METAVIR score F2A2 (B, D, F, H) human liver sections. (A, B): Liver sections stained for CRBP-1 showed that HSCs (arrows) were positively stained in normal and fibrotic liver. (C, D): Liver sections stained for LRAT showed that both HSCs (arrows) and endothelial cells (arrowheads) were positively stained in the normal and fibrotic liver. The inset shows a higher magnification view of a HSC. (E, F): Liver sections stained for smooth muscle actin (SMA) showed that the HSCs in the space of Disse were hardly stained, while the myofibroblasts around the portal area and smooth muscle cells in small arteries in the portal area were positively stained. (G, H): Liver sections stained for neurotrophin-3 (NT-3) showed that HSCs (arrows) were positively stained in the normal and fibrotic liver. (CV; central vein, P; portal vein) magnification: A, C, E, G;  $\times 200$ , B, D, F, H;  $\times 100$ , C (inset);  $\times 1,000$ .

Subsequently, double immunofluorescence staining was evaluated. After antigen retrieval using a microwave, the sections were incubated with the mixture of anti-LRAT antibody labelled with FITC (Invitrogen Corporation, Carlsbad, CA, USA) and anti-CRBP-1 antibody labelled with R-Phycoerythrin (Seikagaku Biobusiness Corporation, Tokyo, Japan) at the same dilutions as described previously for 60 min at room temperature. The sections were lightly washed and mounted with ProLong<sup>®</sup> Gold antifade reagent (Molecular Probes, Eugene, OR, USA). As a negative control, we used Negative Control Rabbit IgG (Biocare Medical, Concord, CA, USA) at the same concentration as the respective antibodies.

Finally, sections were examined by fluorescence microscopy using a Biozero BZ-8000 microscope (Keyence Corporation, Osaka, Japan).

#### Quantitative evaluation of LRAT and CRBP-1 double positive hepatic stellate cells

Quantitative evaluation of double immunofluorescence was performed using a fluorescence microscope (Biozero BZ-8000; Keyence Corporation, Osaka, Japan). After double immunofluorescence staining, the number of LRAT+/CRBP-1+ cells/field was counted in 3 random fields each in the parenchyma, portal area and fibrous septa (only F3, F4) in each case. Each area was automatically measured using a VH analyzer (Keyence Corporation, Osaka, Japan). The average number of LRAT+/CRBP-1+ cells/field was calculated in F0-F4 respectively (Fig. 1).

#### Statistical analysis

Comparisons between the two groups were performed using Student's *t*-test. The difference between groups was considered statistically significant at  $P < 0.05$ .

## Results

#### Immunohistochemical examination of liver specimens

Human liver samples obtained from 24 patients were studied. The samples were from 10 females and 14 males aged 25–83 years (average: 52 years). Livers of various fibrotic stages were classified into F1–F4 according to their METAVIR score, excluding normal livers. The cases of viral hepatitis or cirrhosis were used as pathological liver specimens in order to demonstrate whether HSCs were present in the fibrotic areas around the central vein but also in portal fibrosis.

Human normal and fibrotic liver specimens were immunostained with anti-CRBP-1, anti-LRAT, anti-SMA and anti-NT-3 antibodies. HSCs in the space of Disse were positively stained for both CRBP-1 and LRAT in the normal and fibrotic liver specimens (Fig. 2A–D). In addition, the endothelial cells of the portal vein and

sinusoids were stained with the anti-LRAT antibody (Fig. 2C,D). Smooth muscle actin (SMA), an actin isoform, can be regarded as a good marker for identification of activated HSCs (37). HSCs in the space of Disse were barely stained for SMA, in contrast to the CRBP-1 and LRAT staining, although the myofibroblasts in the portal area and fibrous fascicles were positively stained (Fig. 2E,F). NT-3, a neurotrophic factor, is also regarded to be a marker identifying HSCs (38, 39). In this study, HSCs in the space of Disse were positively stained for NT-3, as well as LRAT and CRBP-1, in the normal and fibrotic liver specimens (Fig. 2G,H).

Double immunostaining for LRAT and SMA in human cirrhotic liver specimens showed that SMA was

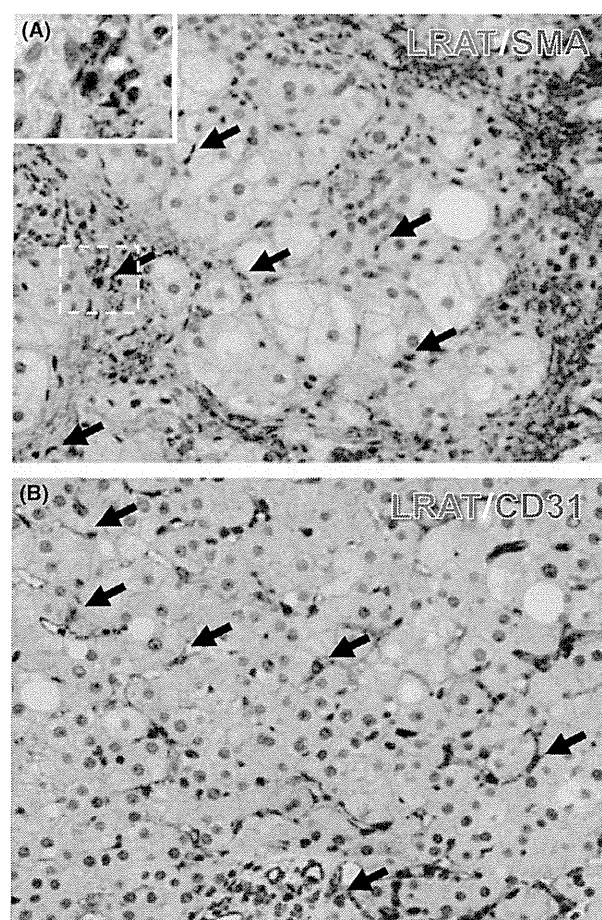


**Fig. 3.** (A) Double immunostaining for LRAT (brown labelling) and SMA (red labelling) of human cirrhotic liver (METAVIR score of F4A2). SMA was positive in the fibrous fascicles. On the other hand, a few LRAT positive cells (arrows) were observed in the parenchyma and fibrous septa. The inset shows a higher magnification view of a HSC which colocalized with LRAT and SMA in fibrous fascicles. (B) Double immunostaining for LRAT (brown labelling) and CD31 (red labelling) of the human liver (METAVIR score of F1A1). CD31 was positive in endothelial cells in the sinusoid and portal area. LRAT was positive in both HSCs (arrows) and endothelial cells in the sinusoid. magnification:  $\times 200$ , inset  $\times 1000$ .

strongly positive in fibrous fascicles, while LRAT was mainly positive in HSCs in the space of Disse. Some of the LRAT positive cells in the fibrous fascicles were colocalized with SMA positive cells (Fig. 3A). Double immunostaining for LRAT and CD31 in the human liver specimens revealed positivity for CD31 in endothelial cells in the sinusoid and portal area and positivity for LRAT in both HSCs (arrows) and endothelial cells in the sinusoid (Fig. 3B).

Double immunostaining for LRAT and CRBP-1 in the human liver specimens showed LRAT+/CRBP-1+ cells in HSCs in the parenchyma (arrows) and myofibroblasts in the portal area (arrowheads) (Fig. 4A). The double immunofluorescence staining for LRAT and CRBP-1 in the human fibrotic liver detected by fluorescence microscopy showed colocalization of both markers in the HSCs in the parenchyma (Fig. 4B–D).

Subsequently, to investigate the relationship between the distribution of LRAT+/CRBP-1+ cells and liver fibrosis, double immunofluorescence staining for LRAT and CRBP-1 was performed for all 24 cases. The number of LRAT+/CRBP-1+ cells/field was counted in 3 random fields each in the parenchyma, portal area and fibrous septa (only F3 and F4) in each case. The numbers in the upper left corner of each image indicate the average number of LRAT+/CRBP-1+ cells/mm<sup>2</sup>. In the parenchyma, the number of LRAT+/CRBP-1+ cells in the space of Disse was not significantly different among F0–F4 (Fig. 5A–E). In the portal area, LRAT+/CRBP-1+

cells were hardly seen in normal liver (Fig. 5F). In F1 and F2, the LRAT+/CRBP-1+ cells were observed mainly at the periphery of the portal area (arrows) (Fig. 5G,H). The number of both positive cells was almost same in F1 and F2. In F3, F4, a large number of double positive cells were seen more than in F1 or F2 (Fig. 5I,J). In addition, in the fibrous septa in F3 and F4, a larger number of positive cells were seen than in the portal area of F3 or F4 (Fig. 5K,L).

Statistical analysis (Fig. 6) showed that the average number of positive cells in the parenchyma was not significantly different. The number of F0 in the portal area was statistically different from the number of F1 to F4 (a-b:  $P < 0.005$ ; a-c:  $P < 0.0002$ ; a-d:  $P < 0.03$ ; a-e:  $P < 0.04$ ). In addition, the average number of double positive cells was increased with the progression of fibrosis. Moreover, the average number of fibrous septa in F3 and F4 was statistically different from that of the portal area in F1 and F2 (b-f:  $P < 0.005$ ; c-f:  $P < 0.003$ ; b-g:  $P < 0.0001$ ).

## Discussion

HSCs in the space of Disse definitively contribute to fibrogenesis in parenchymal injury, such as alcoholic liver disease and non-alcoholic steatohepatitis, by trans-differentiation to activated HSCs (myofibroblasts). On the other hand, the origin of fibrogenic cells associated with portal fibrosis was unclear. Some agree that the

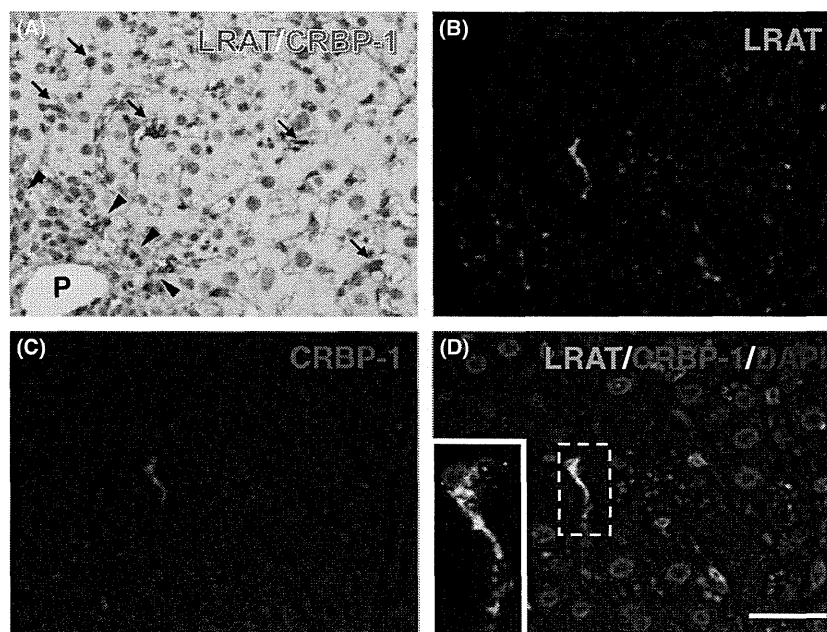


**Fig. 4.** (A) Double immunostaining for LRAT (red labelling) and CRBP-1 (brown labelling) of the human liver (METAVIR score of F2A2). LRAT+/CRBP-1+ cells were observed in HSCs in the parenchyma (arrows) and myofibroblasts in the portal area (arrowheads). (B–D) Double immunofluorescence staining for LRAT (green labelling) and CRBP-1 (red labelling) of human fibrotic liver with a METAVIR score of F2A2. The HSC in the space of Disse showed reactivity for LRAT (B) and CRBP-1 (C), and colocalization of LRAT and CRBP-1 (yellow double labelling) (D). Bar 20  $\mu\text{m}$ .

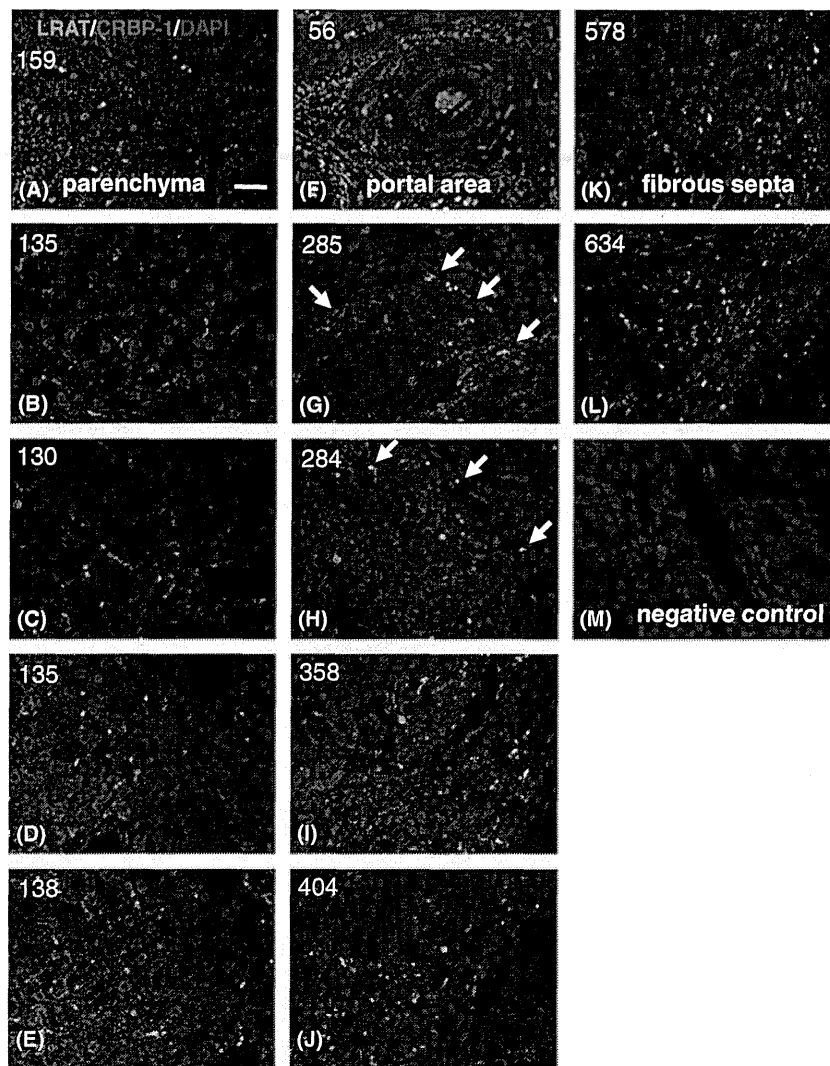


**Fig. 5.** Double immunofluorescence staining for LRAT and CRBP-1 in the parenchyma (A–E), portal area (F–J), and fibrous septa (K, L). The numbers in the upper left corner of each image indicate the average number of LRAT+/CRBP-1+ cells/mm<sup>2</sup>. In the parenchyma, the number of LRAT+/CRBP-1+ cells in the space of Disse was not significantly different among the F0–F4 tissues (A–E). In the portal area, LRAT+/CRBP-1+ cells were hardly seen in the normal liver (F). In the F1 (G) and F2 (H) samples, LRAT+/CRBP-1+ cells were seen mainly at the periphery of the portal area (arrow). The number of both positive cells was almost the same in F1 and F2 tissues. In the F3 (I) and F4 (J) tissues, a large number of double positive cells were seen than in the F1 (G) or F2 (H) tissues. In addition, in the fibrous septa in F3 (K) and F4 (L) tissues, a larger number of positive cells were seen than in the portal area of F3 (I) or F4 (J) tissues. Negative control studies were also done using a Negative Control Rabbit IgG (M). Bar; 20  $\mu$ m.

fibrogenic cells associated with portal fibrosis are portal fibroblasts (6, 40), or the cells derived from bone marrow (2–5); however, a few people believe that the fibrogenic cells are HSCs (41, 42). This study examined the *in situ* distribution of HSCs that expressed LRAT and CRBP-1 proteins was in human normal and pathological livers, particularly those with hepatitis B and C, to determine their contribution to HSCs on portal fibrosis. Some of the cells that coexpressed both LRAT and CRBP-1 were seen in the portal area and fibrous septa, especially in diseased liver. This result suggests that the cells that have the characteristic profile of HSCs can

exist in the fibrous area. This suggests that HSCs in the space of Disse migrate from lobules to the fibrous area or are involved with the fibrous area, since these cells were particularly seen in fibrous expansion of the portal area and fibrous septa than in the portal tracts. These cells represented less than 20% of all cells/field (data not shown). Therefore, HSCs seem to partially contribute to a portal fibrosis. It is possible that cells other than HSCs mainly contributed to portal fibrosis. Ramadori *et al.* reported that the myofibroblasts in the fibrous septa closely resembled the (myo)fibroblasts in the portal field according to an immunohistochemical study using

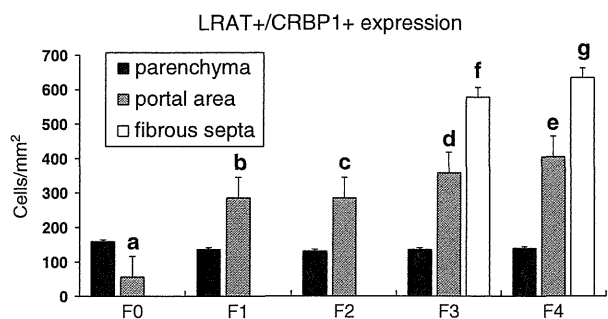


**Fig. 6.** The average ratio of the number of LRAT+/CRBP-1+ cells. The average number of positive cells in the parenchyma (black bars) was not significantly different. The number of F0 in the portal area (grey bars) was statistically different from the number of F1 to F4 (a-b:  $P < 0.005$ ; a-c:  $P < 0.0002$ ; a-d:  $P < 0.03$ ; a-e:  $P < 0.04$ ). In addition, the average number of double positive cells was increased with the progression of fibrosis. Moreover, the average number of fibrous septa (white bar) in F3 and F4 was statistically different from that of the portal area in F1 and F2 respectively (b-f:  $P < 0.005$ ; c-f:  $P < 0.003$ ; b-g:  $P < 0.0001$ ).

*in vivo* HSC markers (6). Portal fibrogenesis may involve HSCs as well as portal fibroblasts.

We observed that the LRAT+/CRBP-1+ cells in the fibrous area did not contain lipid droplets in the cytoplasm, in contrast to the HSCs in the space of Disse. These cells apparently do not store vitamin A. Vitamin A from food absorbed from the small intestine is taken up by hepatocytes (liver parenchymal cells) in the form of retinyl ester through several metabolic steps (20). Retinyl ester is hydrolyzed to retinol again and bound to RBP4 in hepatocytes (43). A high concentration of retinol-bound RBP4 (holo-RBP4) in hepatocytes is secreted into the space of Disse. Excessive retinol likely diffuses into HSCs and becomes bound to CRBP-1. LRAT consists of esterified retinol to retinyl esters packed in lipid droplets in the cytoplasm. This vitamin A storing system is useful for maintaining the plasma retinol level at a nearly constant concentration ( $\sim 1\text{--}3 \times 10^{-6}$  mol/L) (43) to prevent toxicity because of hypervitaminosis A. The concentration of retinol in the space of Disse is apparently higher than that observed in the plasma following its release from hepatocytes after the ingestion of food. However, the concentration of retinol in the fibrous area seems to be similar to the plasma retinol level, since the blood supply in the fibrous area is from the portal veins or hepatic arteries. Since the retinol level as a substrate of LRAT is lower in the fibrous area than in the space of Disse, retinyl ester is not synthesized, even in LRAT+/CRBP-1+ cells. There are vitamin A storing-cells in other organs such as the lung, kidney, intestine and pancreas (7, 44–46). Definite lipid droplets in these sites are never seen under normal conditions, though lipid droplets increase in a rat hypervitaminosis A experimental model (44). In particular, pancreatic stellate cells are

nearly identical to HSCs and both are presumed to share a common origin (47, 48). Stellate cells in other organs do not store vitamin A because of the lack of sufficient retinol as a substrate of LRAT as there is no microenvironment like the space of Disse which presents a high concentration of retinol. This condition is similar to the fibrous area in the human diseased liver under normal vitamin A conditions (normal nutritive status). Moreover, Fonseca *et al.* reported that fat-storing cells appear in the portal area and fibrous septa in chronic hepatitis model using *C. hepatica*-infected rats with hypervitaminosis A (42). This finding is consistent with the hypothesis that stellate cells in lobules migrate to the fibrous area including the portal area and contribute to fibrogenesis when liver damage occurs.

In conclusion, the present results provide direct evidence that the cells coexpressing both LRAT and CRBP-1 proteins contribute in part to the development of portal fibrogenesis in addition to parenchymal fibrogenesis in patients with viral hepatitis.

#### Acknowledgements

**Financial support:** This work was supported in part by grants, from the High Technology Research Center Project for Private University, from The Jikei University Research Fund, and from Grants-in-Aid for Scientific Research (#17590476, #19590572 and #22790673) by the Ministry of Education, Culture, Sports, Science and Technology in Japan, from the Program for Promotion of Fundamental Studies in Health Sciences of the National Institute of Biomedical Innovation (NIBIO), from JSPS Core-to-Core Program, A. Advanced Research Networks, and from the Research on the Innovative Development and the Practical Application of New Drugs for Hepatitis B (Principal investigator: Soichi Kojima; H24-B Drug Discovery-Hepatitis-General-003) provided by the Ministry of Health, Labor and Welfare of Japan (2012).

**Conflicts of interest:** The authors do not have any disclosures to report.

#### References

- Bataller R, Brenner DA. Liver fibrosis. *J Clin Invest* 2005; **115**: 209–18.
- Baba S, Fujii H, Hirose T, *et al.* Commitment of bone marrow cells to hepatic stellate cells in mouse. *J Hepatol* 2004; **40**: 255–60.
- Kisseleva T, Uchinami H, Feirt N, *et al.* Bone marrow-derived fibrocytes participate in pathogenesis of liver fibrosis. *J Hepatol* 2006; **45**: 429–38.
- Forbes SJ, Russo FP, Rey V, *et al.* A significant proportion of myofibroblasts are of bone marrow origin in human liver fibrosis. *Gastroenterology* 2004; **130**: 1807–21.
- Russo FP, Alison MR, Bigger BW, *et al.* The bone marrow functionally contributes to liver fibrosis. *Gastroenterology* 2006; **130**: 1807–21.
- Ramadori G, Saile B. Portal tract fibrogenesis in the liver. *Lab Invest* 2004; **84**: 153–9.

7. Hinz B, Phan SH, Thannickal VJ, et al. The myofibroblast: one function multiple origins. *Am J Pathol* 2007; **170**: 1807–16. 38.
8. Sicklick JK, Choi SS, Bustamante M, et al. Evidence for epithelial-mesenchymal transitions in adult liver cells. *Am J Physiol Gastr Liver Physiol* 2006; **291**: G575–83.
9. Robertson H, Kirby JA, Yip WW, et al. Biliary epithelial-mesenchymal transition in posttransplantation recurrence of primary biliary cirrhosis. *Hepatology* 2007; **45**: 977–81.
10. Zeisberg M, Yang C, Martino M, et al. Fibroblasts derive from hepatocytes in liver fibrosis via epithelial to mesenchymal transition. *J Biol Chem* 2007; **282**: 23337–47.
11. Ikegami T, Zhang Y, Matsuzaki Y. Liver fibrosis: possible involvement of EMT. *Cells Tissues Organs* 2007; **185**: 213–21.
12. Zeisberg EM, Tarnavski O, Zeisberg M, et al. Endothelial-to-mesenchymal transition contributes to cardiac fibrosis. *Nat Med* 2007; **13**: 952–61.
13. Iwaisako K, Brenner D, Kisseleva T. What's new in liver fibrosis? The origin of myofibroblasts in liver fibrosis. *J Gastroen Hepatol* 2012; **27**: 65–8.
14. Yost RW, Harrison EH, Ross AC. Esterification of retinol bound to cellular retinol-binding protein. *J Biol Chem* 1988; **263**: 18693–701.
15. Matsuura T, Gad MZ, Harrison EH, Ross AC. Lecithin: retinol acyltransferase and retinyl ester hydrolase activities are differentially regulated by retinoids and have distinct distributions between hepatocyte and nonparenchymal cell fractions of rat liver. *J Nutr* 1997; **127**: 218–24.
16. Saari JC, Bredberg DL, Farrell DF. Retinol esterification in bovine retinal pigment epithelium: reversibility of lecithin: retinol acyltransferase. *Biochem J* 1993; **291**: 697–700.
17. Kurlandsky SB, Duell EA, Kang S, Voorhees JJ, Fisher GJ. Auto-regulation of retinoic acid biosynthesis through regulation of retinol esterification in human keratinocytes. *J Biol Chem* 1996; **271**: 15346–52.
18. Zolfaghari R, Ross AC. Lecithin: retinol acyltransferase expression is regulated by dietary vitamin A and exogenous retinoic acid in the lung of adult rats. *J Nutr* 2002; **132**: 1160–4.
19. Shingleton JL, Skinner MK, Ong DE. Retinol esterification in Sertoli cells by lecithin: retinol acyltransferase. *Biochemistry* 1989; **28**: 9647–53.
20. Ong DE, Lucas PC, Kakkad B, Quick TC. Ontogeny of two vitamin A-metabolizing enzymes and two retinol-binding proteins present in the small intestine of the rat. *J Lipid Res* 1991; **32**: 1521–7.
21. Randolph RK, Ross AC. Vitamin A status regulates hepatic lecithin: retinol acyltransferase activity in rats. *J Biol Chem* 1991; **266**: 16453–7.
22. Matsuura T, Ross AC. Regulation of hepatic lecithin: retinol acyltransferase activity by retinoic acid. *Arch Biochem Biophys* 1993; **301**: 221–7.
23. Shimada T, Ross AC, Muccio DD, Brouillette WJ, Shealy YF. Regulation of hepatic lecithin: retinol acyltransferase activity by retinoic acid receptor-selective retinoids. *Arch Biochem Biophys* 1997; **344**: 220–7.
24. Nagatsuma K, Hayashi Y, Hano H, et al. Lecithin: retinol acyltransferase protein is distributed in both hepatic stellate cells and endothelial cells of normal rodent and human liver. *Liver Int* 2009; **29**: 47–54.
25. Kato M, Blaner WS, Mertz JR, et al. Influence of retinoid nutritional status on cellular retinol- and cellular retinoic acid-binding protein concentrations in various rat tissues. *J Biol Chem* 1985; **260**: 4832–8.
26. Rajan N, Blaner WS, Soprano DR, Sahara A, Goodman DS. Cellular retinol-binding protein messenger RNA levels in normal and retinoid-deficient rats. *J Lipid Res* 1990; **31**: 821–9.
27. Blomhoff R, Rasmussen M, Nilsson A, et al. Hepatic retinol metabolism distribution of retinoids, enzymes, and binding proteins in isolated rat liver cells. *J Biol Chem* 1985; **260**: 13560–5.
28. Blomhoff R, Wake K. Perisinusoidal stellate cells of the liver: important roles in retinol metabolism and fibrosis. *FASEB J* 1991; **5**: 271–7.
29. Ong DE, MacDonald PN, Gubitosi AM. Esterification of retinol in rat liver: possible participation by cellular retinol-binding protein and cellular retinol-binding protein II. *J Biol Chem* 1988; **263**: 5789–96.
30. Herr FM, Ong DE. Differential interaction of lecithin:retinol acyltransferase with cellular retinol binding proteins. *Biochemistry* 1992; **31**: 6748–55.
31. Kato M, Kato K, Goodman DS. Immunocytochemical studies on the localization of plasma and of cellular retinol-binding proteins and of transthyretin (prealbumin) in rat liver and kidney. *J Cell Biol* 1984; **98**: 1696–704.
32. Eriksson U, Das K, Busch C, et al. Cellular retinol-binding protein quantitation and distribution. *J Cell Biol* 1984; **259**: 13464–70.
33. Uchino K, Tuchweber B, Manabe N, et al. Cellular retinol-binding protein-1 expression and modulation during in vivo and in vitro myofibroblastic differentiation of rat hepatic stellate cells and portal fibroblasts. *Lab Invest* 2002; **82**: 619–28.
34. Lepreux S, Bioulac-Sage P, Gabbiani G, et al. Cellular retinol-binding protein-1 expression in normal and fibrotic/cirrhotic human liver: different patterns of expression in hepatic stellate cells and (myo) fibroblast subpopulations. *J Hepatol* 2004; **40**: 774–80.
35. Rossen EV, Borghet SV, Grunsvan LA, et al. Vinculin and cellular retinol-binding protein-1 are markers for quiescent and activated hepatic stellate cells in formalin-fixed paraffin embedded human liver. *Histochem Cell Biol* 2008; **131**: 313–25.
36. Bedossa P, Poynard T. An algorithm for the grading of activity in chronic hepatitis C. The METAVIR Cooperative Study Group. *Hepatology* 1996; **24**: 289–93.
37. Schmitt-Graff A, Kruger S, Bochar F, Gabbiani G, Denk H. Modulation of alpha smooth muscle actin and desmin expression in perisinusoidal cells of normal and diseased human livers. *Am J Pathol* 1991; **138**: 1233–42.
38. Cassiman D, Libbrecht L, Desmet V, Deneef C, Roskams T. Hepatic stellate cell/myofibroblast subpopulations in fibrotic human and rat livers. *J Hepatol* 2002; **36**: 200–9.
39. Cassiman D, Roskams T. Beauty is in the eye of the beholder: emerging concepts and pitfalls in hepatic stellate cell research. *J Hepatol* 2002; **37**: 527–35.
40. Beaussier M, Wendum D, Schiffer E, et al. Prominent contribution of portal mesenchymal cells to liver fibrosis in ischemic and obstructive cholestatic injuries. *Lab Invest* 2007; **87**: 292–303.

41. Marra F, Romanelli RG, Giannini C, *et al.* Monocyte chemotactic protein-1 as a chemoattractant for human hepatic stellate cells. *Hepatology* 1999; **29**: 140–8.
42. Fonseca YO, Lima CB, Santos ET, Andrade ZA. On the presence of hepatic stellate cells in portal spaces. *Mem Inst Oswaldo Cruz* 2005; **100**: 289–91.
43. Ross AC. Cellular metabolism and activation of retinoids: roles of cellular retinol-binding proteins. *FASEB J* 1993; **7**: 317–27.
44. Nagy NE, Holven KB, Roos N, *et al.* Storage of vitamin A in extrahepatic stellate cells in normal rats. *J Lipid Res* 1997; **38**: 645–58.
45. Wake K. 'Sternzellen' in the liver: perisinusoidal cells with special reference to storage of vitamin A. *Am J Anat* 1971; **132**: 429–62.
46. Omary MB, Lugea A, Lowe AW, Pandol SJ. The pancreatic stellate cell: a star on the rise in pancreatic diseases. *J Clin Invest* 2007; **117**: 50–9.
47. Buchholz M, Kestler HA, Holzmann K, *et al.* Transcriptome analysis of human hepatic and pancreatic stellate cells: organ-specific variations of a common transcriptional phenotype. *J Mol Med* 2005; **83**: 795–805.
48. Erkan M, Weis N, Pan Z, *et al.* Organ-, inflammation- and cancer specific transcriptional fingerprints of pancreatic and hepatic stellate cells. *Mol Cancer* 2010; **9**: 88.

# High ubiquitous mitochondrial creatine kinase expression in hepatocellular carcinoma denotes a poor prognosis with highly malignant potential

Baasanjav Uranbileg<sup>1\*</sup>, Kenichiro Enooku<sup>1,2\*</sup>, Yoko Soroida<sup>1</sup>, Ryunosuke Ohkawa<sup>1</sup>, Yotaro Kudo<sup>2</sup>, Hayato Nakagawa<sup>2</sup>, Ryosuke Tateishi<sup>2</sup>, Haruhiko Yoshida<sup>2</sup>, Seiko Shinzawa<sup>2</sup>, Kyoji Moriya<sup>3</sup>, Natsuko Ohtomo<sup>2</sup>, Takako Nishikawa<sup>2</sup>, Yukiko Inoue<sup>2</sup>, Tomoaki Tomiya<sup>2</sup>, Soichi Kojima<sup>4</sup>, Tomokazu Matsuura<sup>5</sup>, Kazuhiko Koike<sup>2</sup>, Yutaka Yatomi<sup>1</sup> and Hitoshi Ikeda<sup>1,2</sup>

<sup>1</sup>Department of Clinical Laboratory Medicine, Graduate School of Medicine, The University of Tokyo, Tokyo, Japan

<sup>2</sup>Department of Gastroenterology, Graduate School of Medicine, The University of Tokyo, Tokyo, Japan

<sup>3</sup>Department of Infection Control and Prevention, Graduate School of Medicine, The University of Tokyo, Tokyo, Japan

<sup>4</sup>Micro-signaling Regulation Technology Unit, RIKEN Center for Life Science Technologies, Wako, Saitama, Japan

<sup>5</sup>Department of Laboratory Medicine, The Jikei University School of Medicine, Tokyo, Japan

We previously reported the increased serum mitochondrial creatine kinase (MtCK) activity in patients with hepatocellular carcinoma (HCC), mostly due to the increase in ubiquitous MtCK (uMtCK), and high uMtCK mRNA expression in HCC cell lines. We explored the mechanism(s) and the relevance of high uMtCK expression in HCC. In hepatitis C virus core gene transgenic mice, known to lose mitochondrial integrity in liver and subsequently develop HCC, uMtCK mRNA and protein levels were increased in HCC tissues but not in non-tumorous liver tissues. Transient overexpression of ankyrin repeat and suppressor of cytokine signaling box protein 9 (ASB9) reduced uMtCK protein levels in HCC cells, suggesting that increased uMtCK levels in HCC cells may be caused by increased gene expression and decreased protein degradation due to reduced ASB9 expression. The reduction of uMtCK expression by siRNA led to increased cell death, and reduced proliferation, migration and invasion in HCC cell lines. Then, consecutive 105 HCC patients, who underwent radiofrequency ablation with curative intent, were enrolled to analyze their prognosis. The patients with serum MtCK activity >19.4 U/L prior to the treatment had significantly shorter survival time than those with serum MtCK activity ≤19.4 U/L, where higher serum MtCK activity was retained as an independent risk for HCC-related death on multivariate analysis. In conclusion, high uMtCK expression in HCC may be caused by hepatocarcinogenesis *per se* but not by loss of mitochondrial integrity, of which ASB9 could be a negative regulator, and associated with highly malignant potential to suggest a poor prognosis.

**Key words:** ubiquitous mitochondrial creatine kinase, ankyrin repeat and suppressor of cytokine signaling box protein 9, hepatocellular carcinoma, prognostic factor

**Abbreviations:** AFP: alpha-fetoprotein; ALT: alanine aminotransferase; ASB: ankyrin repeat and suppressor of cytokine signaling box protein; AST: aspartate aminotransferase; DCP: des-gamma-carboxy prothrombin; GGT: gamma-glutamyltransferase; HCC: hepatocellular carcinoma; HCV: hepatitis C virus; RFA: radiofrequency ablation; ROC: receiver operating characteristic; SOCS: suppressor of cytokine signaling; uMtCK: ubiquitous mitochondrial creatine kinase

\*B.U. and K.E. contributed equally to this work

DOI: 10.1002/ijc.28547

**History:** Received 2 July 2013; Accepted 1 Oct 2013; Online 15 Oct 2013

**Correspondence to:** Hitoshi Ikeda, Department of Clinical Laboratory Medicine, Graduate School of Medicine, The University of Tokyo, 7-3-1 Hongo, Bunkyo-ku, Tokyo 113-8655, Japan, Tel.: +81-3-3815-5411, Fax: +81-3-5689-0495, E-mail: ikeda-1im@h.u-tokyo.ac.jp

Primary liver cancer, 95% of which is hepatocellular carcinoma (HCC), is ranked third in men and fifth in women as a cause of death from malignant neoplasms in Japan.<sup>1</sup> Furthermore, the worldwide incidence of HCC has increased over several decades, and HCC has recently received considerable attention as a common cause of mortality.<sup>2</sup> HCC often arises in background of liver cirrhosis, which is formed as a result of chronic viral infections, alcoholic injury and some other disorders in the liver.<sup>3,4</sup> Of note, HCC has recently been linked to non-alcoholic fatty liver disease, and this association may contribute to the rising incidence of HCC witnessed in many industrialized countries. It is also problematic that HCC may complicate non-cirrhotic, non-alcoholic fatty liver disease with mild or absent fibrosis, greatly expanding the population potentially at higher risk.<sup>5</sup> Because HCC has a poor prognosis due to its aggressive nature, surgical resection and radiofrequency ablation (RFA) are effective only in early stage of HCC.<sup>4,6</sup> Recurrence occurs almost in 70% of patients with HCC of the first occurrence within 5 years.<sup>7</sup> Regarding the treatment of HCC in United



**What's new?**

The identification of biomolecules associated with hepatocellular carcinoma (HCC) could greatly improve screening for early disease detection. Ubiquitous mitochondrial creatine kinase (uMtCK) could be a promising marker in this context, though its relevance in HCC is unclear, as it may be associated with mitochondrial stability rather than carcinogenesis. Here, in transgenic mice susceptible to the loss of liver mitochondrial integrity, uMtCK was found to be elevated in HCC tissue but not in non-tumorous liver tissue. Increased uMtCK was further linked to reduced expression of ASB9 and elevated risk for HCC-related death.

States veterans, approximately 40% of patients were reportedly diagnosed during hospitalization. Most patients were not seen by a surgeon or oncologist for treatment evaluation and only 34% received treatment.<sup>8</sup> Although there was no effective chemotherapy for advanced HCC for a long time, a novel anti-cancer therapy such as anti-angiogenesis pathway therapy has just recently been developed to prolong survival in patients with the advanced disease.<sup>9,10</sup> However, its effect is rather limited, just extending median survival from 7.9 months to 10.7 months in patients with advanced HCC.<sup>10</sup> Thus, the effective way for early detection of HCC is urgently needed. To this end, the recommended screening strategy for patients with cirrhosis includes the determination of serum alpha-fetoprotein (AFP) levels and an abdominal ultrasound every 6 months to detect HCC at an earlier stage. AFP, however, is a marker characterized by poor sensitivity and specificity.<sup>11</sup> Although other potential markers such as des-gamma-carboxy prothrombin (DCP) and squamous cell carcinoma antigen-immunoglobulin M complex have been proposed to use for diagnosis of HCC, none of them is optimal; however, when used together, their sensitivity in detecting HCC is increased.<sup>11–14</sup> For cholangiocarcinoma, which is a relatively rare type of primary liver cancer that originates in the bile duct epithelium, carbohydrate antigen 19-9, carcinogenic embryonic antigen and cancer antigen 125 have shown sufficient sensitivity and specificity to detect and monitor it. In particular, the combination of these markers seems to increase their efficiency in diagnosing of cholangiocarcinoma.<sup>15</sup>

In this context, we have recently reported that serum mitochondrial creatine kinase (MtCK) activity is increased in patients with HCC, even in those with early stage, suggesting that MtCK may be useful to detect early stage of HCC.<sup>16</sup> Among two tissue-specific isozymes of MtCK, that is, ubiquitous MtCK (uMtCK) and sarcomeric MtCK, we have found that the increase in serum MtCK activity in HCC patients was mostly due to that in serum uMtCK activity but not in serum sarcomeric MtCK activity.<sup>16</sup> Then, we have further observed the higher expression of uMtCK mRNA in HCC cell lines than in normal human liver tissues.<sup>16</sup> Of note, the increased uMtCK expression occurred not only upon malignant changes in the liver, but also in several other malignant tumors such as gastric cancer, breast cancer and lung cancer, where the high expression of uMtCK suggests a poor prognosis.<sup>17–19</sup> In contrast, uMtCK was down-regulated in oral squamous cell carcinoma,<sup>20</sup> and sarcomeric MtCK was

also down-regulated during sarcoma development in leg muscle in mice.<sup>21</sup> Therefore, we aimed to elucidate the mechanism(s) and the significance of high uMtCK expression in HCC in this study.

We first examined whether loss of mitochondrial integrity might be involved in high uMtCK expression in HCC, using hepatitis C virus (HCV) core gene transgenic mice. HCV core protein has been first demonstrated to play a pivotal role in HCC development within these transgenic mice, which are known to lose mitochondrial integrity and subsequently develop HCC without apparent inflammation and fibrosis in the liver.<sup>22,23</sup> As a regulatory factor for uMtCK expression, we have focused on the ankyrin repeat and suppressor of cytokine signaling (SOCS) box protein (ASB) family, which reportedly plays an important role in biological processes and regulations of cell proliferation and differentiation. The ASBs have two functional domains: a SOCS box and a variable number of N-terminal ankyrin repeats. Although SOCS domain uses the SH2 domain to recruit substrates, the ankyrin repeat regions serve as a specific protein-protein interaction domain to recruit target substrates.<sup>24</sup> One of ASB family protein, ASB9, was found to interact with brain type of creatine kinase, leading to its degradation.<sup>25</sup> Recently, uMtCK was found to be another ASB9 target.<sup>26</sup> Ankyrin repeat domains of ASB9 associates with the substrate binding site of uMtCK and induce its ubiquitination. Thus, we analyzed the potential association between uMtCK and ASB9 in HCC cell lines, HepG2, PLC/PRF/5, HuH7, in which the expression of uMtCK mRNA was shown to be increased compared with normal liver tissues.<sup>16</sup> To clarify the significance of high uMtCK expression in HCC, we used the siRNA approach to silence uMtCK expression and study its effects on HCC cell lines. Finally, we analyzed the clinical significance of high uMtCK expression in HCC patients who were treated with RFA.

**Material and Methods****Materials**

Human normal liver RNA was purchased from Cell Applications (San Diego, CA), and human whole liver cell pellets from DV Biologics (Costa Mesa, CA). Specific antibodies against uMtCK and ASB9 were obtained from Abcam (Cambridge, UK), an antibody against caspase 3 from Cell Signaling Technology (3G2; Boston, MA), and an antibody against beta-actin from Sigma-Aldrich (MO).

### Cells and cell culture

HCC cell lines, HepG2 and PLC/PRF/5 were obtained from RIKEN BioResource Center (Tsukuba, Ibaraki, Japan) and HuH7 from Health Science Research Resources Bank, Japan Health Science Foundation. HepG2 and PLC/PRF/5 were maintained in RPMI-1640 containing 10% of fetal bovine serum, and HuH7, in Dulbecco's Modified Eagle Medium containing 10% of fetal bovine serum.

### Transgenic mice

HCV core gene transgenic mice were produced as previously described.<sup>22</sup> Nontransgenic littermates of the transgenic mice were used as controls. All mice were fed a standard pelleted diet and water *ad libitum* under normal laboratory conditions of 12 hr-light/dark cycles, and received humane care. The experimental protocol was approved by Animal Research Committee of the University of Tokyo.

### Quantitative real-time PCR

Total RNA of HCC cell lines (HepG2, PLC/PRF/5 and HuH7), human normal liver and livers from non-transgenic and HCV core gene transgenic mice were extracted using TRIzol reagent (Invitrogen, CA). One microgram of purified total RNA was transcribed using a SuperScript<sup>TM</sup> First-Strand Synthesis System for RT-PCR (Invitrogen). Quantitative real-time PCR was performed with a LightCycler FastStart DNA Master SYBR Green I kit (Roche Molecular Diagnostics, CA) or TaqMan Universal Master Mix. The primer pairs used were as follows: human ASB9: 5'-CCTGGCATCAGGCTTCTTTC-3' and 5'-ACCCCTGGCTGATGAGGTTTC-3'<sup>27</sup>; human beta-actin: 5'-GGGTCAGAAGGATTCCTATG-3' and 5'-CCTTAATGTCACGCAGATTT-3'.<sup>26</sup> Mouse uMtCK primers and probe were obtained from Applied Biosystems, TaqMan Gene Expression Assays (Mm00438221\_m1). The samples were incubated for 10 min at 95°C, followed by 40 cycles at 95°C for 10 sec, 60°C for 10 sec and 72°C for 10 sec. The target gene mRNA expression level was relatively quantified to beta-actin using 2<sup>-ΔΔCt</sup> method (Applied Biosystems, User Bulletin No 2).

### ASB9 transfection

Cells, transiently expressing human ASB9 protein, were constructed using mammalian cell expression vector p3FLAG CMV-10 containing the corresponding cDNA which derived from human normal liver RNA. The primers used for cloning were 5'-GCGGATCCGTCATGGATGGCAAACAAGGG-3' and 5'-GAGCGGCCGCTTAAGATGTAGGAGAACTGTT-3' which were designed based on human ASB9 reference sequence (NM\_001031739.2). The ASB9 cDNA was created by PCR and verified by DNA sequencing.

### Immunoblot analysis

Cell and tissue extracts were prepared using M-PER Mammalian Protein Extraction Reagent (Thermo Fisher Scientific, IL) plus Halt<sup>TM</sup> Protease Inhibitor Cocktail (Thermo Fisher

Scientific). Immunoblot analysis was performed as previously described,<sup>28</sup> using NuPAGE SDS-PAGE Gel (Invitrogen) and iBlot Dry Blotting System (Invitrogen) with specific antibodies against uMtCK (dilution 1:1,000), ASB9 (dilution 1:500), caspase 3 (dilution 1:1,000) and beta-actin (dilution 1:2,000). Immunoreactive proteins were visualized using a chemiluminescence kit (GE Healthcare, Buckinghamshire, UK), and recorded using a LAS-4000 image analyzer (Fuji Film, Tokyo, Japan). The intensities of immunodetected bands were quantified with NIH Image J software.

### uMtCK siRNA transfection

Cells were transfected with the human uMtCK-specific 23/27mer RNA duplex or a universal negative control duplex at 20 nM, respectively, according to the venter instructions (Integrated DNA Technologies, IA). The human uMtCK-specific RNA duplex used was 5'-UGAAGCACACCACGGAUCU-3' and 3'-ACUUCGUGUGGUGCCUAGA-5',<sup>29</sup> negative control RNA duplex, 5'-CGUUAUUCGCGUAUAAUACGCGUAT-3' and 3'-CAGCAAUUAGCGCAUUAUUAUGCGCAUA-5' (Integrated DNA Technologies). The transfection was performed using Lipofectamine Plus<sup>TM</sup> (Invitrogen) as described.<sup>29</sup>

### Cell membrane integrity and proliferation assays

Cell membrane integrity was determined using the In Vitro Toxicology Assay Kit, Lactic Dehydrogenase based (Sigma-Aldrich). HCC cell lines were inoculated in six-well plates at  $2.5 \times 10^5$  cells/well and cultured for 24 hr before uMtCK siRNA or universal negative control transfection. Dead cells were assessed at 48 hr after transfection.

Cell proliferation in HCC cell lines was measured at 48 hr after transfection with uMtCK siRNA or universal negative control by determination of BrdU incorporation using the Cell Proliferation ELISA, BrdU colorimetric assay (Roche Applied Science, Upper Bavaria, Germany). In the above two assays, absorbance was measured by plate reader (SPECTRA Thermo, TECAN, Männedorf, Switzerland).

### Cell migration and invasion assays

Cell migration and invasion assays were performed according to the venter's instruction (BD, NJ). Cells transfected with uMtCK siRNA or universal negative control were cultured for 24 hr, then  $2 \times 10^4$  cells were plated into the upper chamber of 24-well plates with 8 μm of pore size in serum-starved condition to examine cell migration and polycarbonate transwell filter chamber coated with Matrigel (BD BioCoat Matrigel Invasion Chamber) to check cell invasion. In both assays, 750 μL medium supplemented with 10% serum was added into the lower chambers. Cells were incubated at 37°C for 22 hr, and the inside chambers were removed with cotton swabs and cells that had transferred to the lower membrane surface were fixed and stained with Diff-Quik stain. Cell counts (four random 100× fields per well) are expressed as the mean number of cells per field of view.

### Patients and measurement of MtCK activity

Consecutive 147 HCC patients with cirrhosis caused by hepatitis B virus or HCV, who were admitted into the Department of Gastroenterology, the University of Tokyo Hospital, Tokyo, Japan, between January and April 2010, were previously enrolled to analyze serum MtCK activity.<sup>16</sup> Diagnosis of cirrhosis was based on the presence of clinical and laboratory features indicating portal hypertension, and diagnosis of HCC was made by dynamic CT or MRI.<sup>30,31</sup> Prior to the treatment of HCC, serum MtCK activity was measured<sup>16</sup> with an immuno-inhibition method using the two types of anti-MtCK monoclonal antibodies.<sup>32</sup> Among these patients, 105 patients, who had been successfully treated by RFA without residual HCC after the treatment, were enrolled in the current prognosis analysis. The detailed procedure of RFA has been meticulously described elsewhere.<sup>33</sup> Overall survival of these 105 patients was analyzed from the time of measurement of serum MtCK activity to death related to HCC, excluding the death not associated with HCC expansion or liver insufficiency, such as cardiovascular events or other organ malignancy, or to March 2013.

This study was performed in accordance with the ethical guidelines of the 1975 Declaration of Helsinki and was approved by the Institutional Research Ethics Committees of the authors' institutions. A written informed consent was obtained for the use of the samples in this study.

### Statistical analysis

The results of *in vitro* experiments are expressed as the means and standard error of the mean. Student's *t* test (two tailed) was used for comparison unless indicated otherwise. The results were considered significant when *p*-values were 0.05. In the analysis of risk factors for HCC-related death, we tested the following variables obtained at the time of entry on the univariate and multivariate Cox proportional hazard regression analysis: age, sex, hepatitis B infection, serum MtCK activity, serum albumin concentration, aspartate aminotransferase (AST) levels, alanine aminotransferase (ALT) levels, gamma-glutamyltransferase (GGT) levels, total bilirubin concentration, AFP concentration, DCP concentration, platelet count, prothrombin activity and liver stiffness values. Survival and recurrence curves were created using Kaplan-Meier method and compared *via* log-rank test. Data processing and analysis were performed using S-PLUS 2000 (Math-Soft, Seattle, WA) and SAS Software version 9.1 (SAS Institute, Cary, NC).

## Results

### Loss of mitochondrial integrity may not contribute to high expression of uMtCK in HCC

Mutations of mitochondrial DNA have been reported to be involved in hepatocarcinogenesis in humans.<sup>34,35</sup> Furthermore, in a mouse model for hepatocarcinogenesis, oxidative stress was shown to lead to loss of mitochondrial integrity in

the liver and ultimately hepatocarcinogenesis.<sup>23</sup> Thus, we wondered whether loss of mitochondrial integrity in the liver might be associated with increased expression of uMtCK in HCC. To examine this idea, we used a transgenic mouse model of HCC in HCV infection (transgenic line S-N/863), with which the direct association between HCV and HCC was first described.<sup>22</sup> In these HCV core gene transgenic mice, loss of mitochondrial integrity has been reported to be observed as early as 2 months of age and increased in an age-dependent manner,<sup>23</sup> and ultimately HCC develops at 19 months of age without apparent inflammation or fibrosis in the liver.<sup>22</sup>

We examined uMtCK mRNA levels in the liver of these HCV core protein transgenic mice at 6 months and 19 months of age. These mice at 6 months of age reportedly develop hepatic steatosis<sup>22</sup> as well as loss of mitochondrial integrity.<sup>23</sup> In these mice at 19 months of age, tumor tissues of HCC and non-tumorous tissues of the liver were analyzed. Non-transgenic mice at 6 months of age were used as control. uMtCK mRNA levels were increased in tumor tissues of HCC in HCV core gene transgenic mice at 19 months of age by 7.7-fold compared to the liver tissues of control mice (*p* = 0.02; Fig. 1a). In these HCV core transgenic mice at 19 months of age, uMtCK protein expression was detected in HCC tissues but not in non-tumorous tissues by immunoblot analysis (Fig. 1b). These results suggest that hepatocarcinogenesis *per se* but not loss of mitochondrial integrity may contribute to the increase in uMtCK levels in HCC.

### Transient expression of ASB9 negatively regulates uMtCK protein levels in HCC cells

It has been reported that ASB protein family is importantly involved in ubiquitination-mediated proteolysis pathway and each member of this large protein family has a different target to be degraded. In ASB protein family, we paid attention to ASB9, which reportedly plays a crucial role in the regulation of the brain type of creatine kinase and uMtCK. HCC cell lines, HepG2, PLC/PRF/5 and HuH7, were selected for *in vitro* experiments, because they had been reported to express high levels of uMtCK mRNA compared to human normal liver tissue.<sup>16</sup> To study whether ASB9 could regulate uMtCK protein levels in these HCC cells, we first measured ASB9 mRNA expression in those cells. Figure 2a demonstrates the low ASB9 mRNA expression in HCC cell lines, contrasting with high uMtCK mRNA expression levels in those cells.<sup>16</sup> In line with our mRNA expression data, ASB9 protein levels were almost undetectable in HepG2, PLC/PRF/5 and HuH7 cells comparing to normal whole liver cell pellets (Fig. 2b). Further, we investigated the effect of transient overexpression of ASB9 on uMtCK protein levels in HepG2, PLC/PRF/5 and HuH7 cells. Cells were transiently transfected with mammalian cell expression vector p3FLAG-CMV10 containing human ASB9 DNA and harvested at 36 hr after transfection to analyze protein levels. Down-regulation of uMtCK protein levels by transient

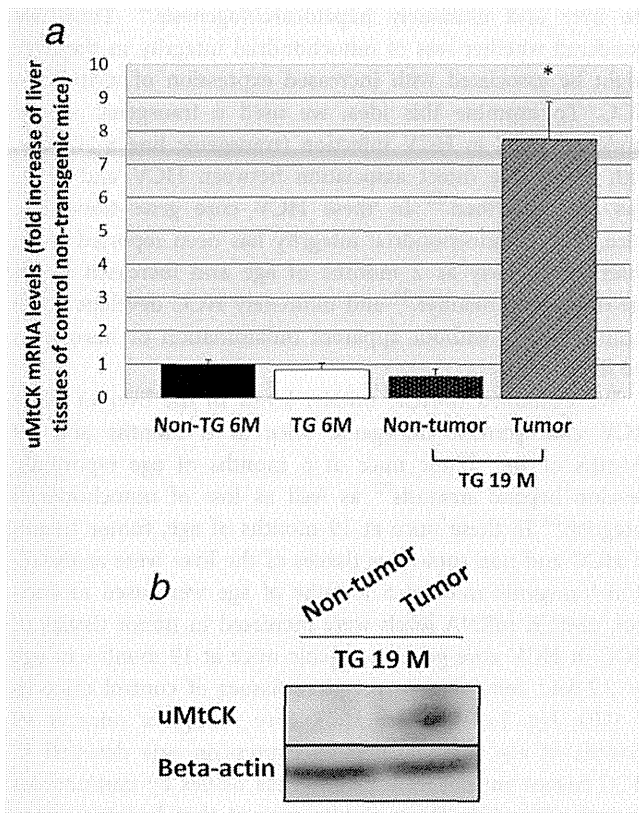


**Figure 1.** uMtCK mRNA and protein levels in liver tissues of the control non-transgenic, HCV core gene transgenic mice. (a) uMtCK mRNA levels were examined by real-time PCR in liver tissues of the control non-transgenic mice (Non-TG) at 6 months of age ( $n = 4$ ), and HCV core gene transgenic mice (TG) at 6 ( $n = 4$ ) and 19 months of age ( $n = 4$ ). For HCV core gene transgenic mice at 19 months of age, HCC tissues and non-tumorous tissues were separately evaluated. Results represent a fold increase level of liver tissues of control non-transgenic mice. An asterisk indicates a significant difference ( $p = 0.02$ ) from liver tissues of non-transgenic mice. (b) uMtCK protein levels were analyzed by immunoblotting in HCC tissues and non-tumorous tissues in the livers of HCV core gene transgenic mice at 19 months of age.

overexpression of ASB9 was observed significantly in HuH7 cells ( $p = 0.007$ ), and a trend of decreased uMtCK protein levels was found in HepG2 and PLC/PRF/5 cells, although not statistically significant (Fig. 2c). These results suggest a functional interaction of ASB9 with uMtCK may lead to degradation of uMtCK protein in HCC cell lines, as previously described.<sup>26</sup>

**Reduction in uMtCK expression led to increased cell death, and reduced proliferation, migration and invasion of HCC cells**

To inhibit high uMtCK expression in HepG2, PLC/PRF/5 and HuH7 cells,<sup>16</sup> isoform-specific siRNA was chosen as described<sup>29</sup> and successfully silenced target protein expression; the results from immunoblot analysis of untransfected and transfected cell lysates with universal negative control and uMtCK siRNA are shown in Figure 3a. As expected, in

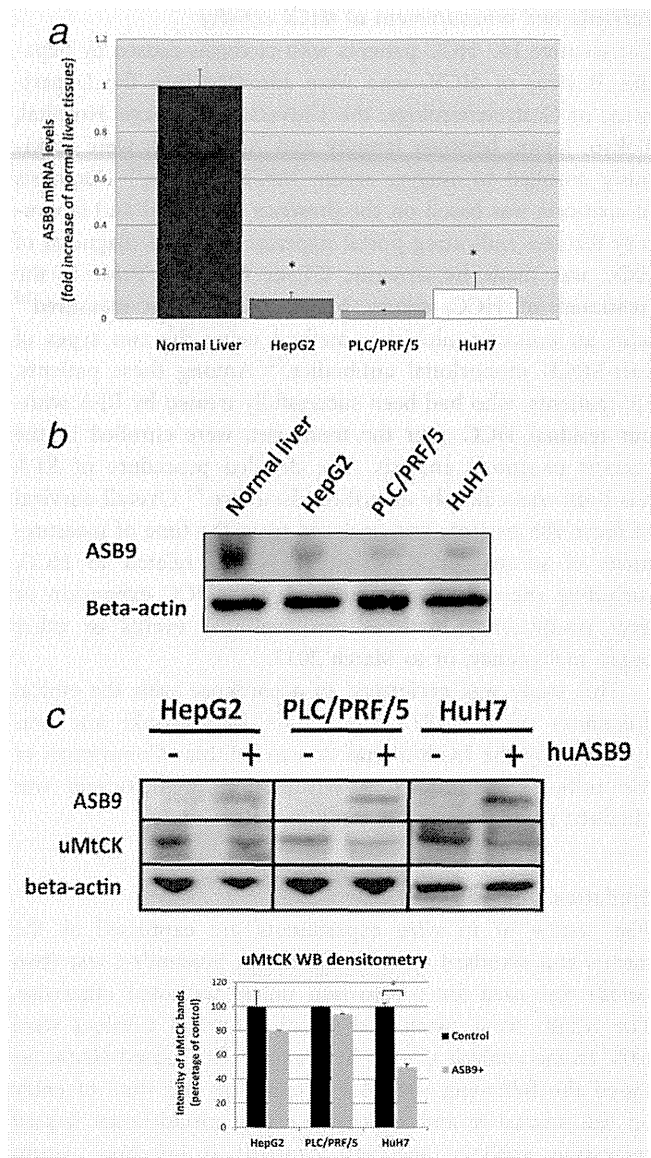


**Figure 2.** ASB9 expression and the effect of ASB9 transfection on uMtCK protein levels in HCC cells. ASB9 mRNA (a) and protein (b) levels in HepG2, PLC/PRF/5 and HuH7 cells were examined by real-time PCR and immunoblot analysis, respectively. As a positive control for ASB9 mRNA and protein expressions, human normal liver RNA and human whole liver cell pellets were used. An asterisk indicates a significant difference from normal liver tissue;  $p = 0.006$  for HepG2,  $p = 0.005$  for PLC/PRF/5 and  $p = 0.01$  for HuH7. Increased expression of ASB9 by transfection caused reduced protein levels of uMtCK in HepG2, PLC/PRF/5 and HuH7 cells (c). An asterisk indicates a significant difference ( $p = 0.007$ ) from control without ASB9 transfection.

all HCC cell lines transfected with uMtCK siRNA, the expression levels of uMtCK were clearly reduced at 36 hr after transfection (Fig. 3a).

Then, the effects of a reduction in uMtCK expression on cell membrane integrity and proliferation were determined in HepG2, PLC/PRF/5 and HuH7 cells. In the first step, we have checked cell membrane integrity by measuring lactate

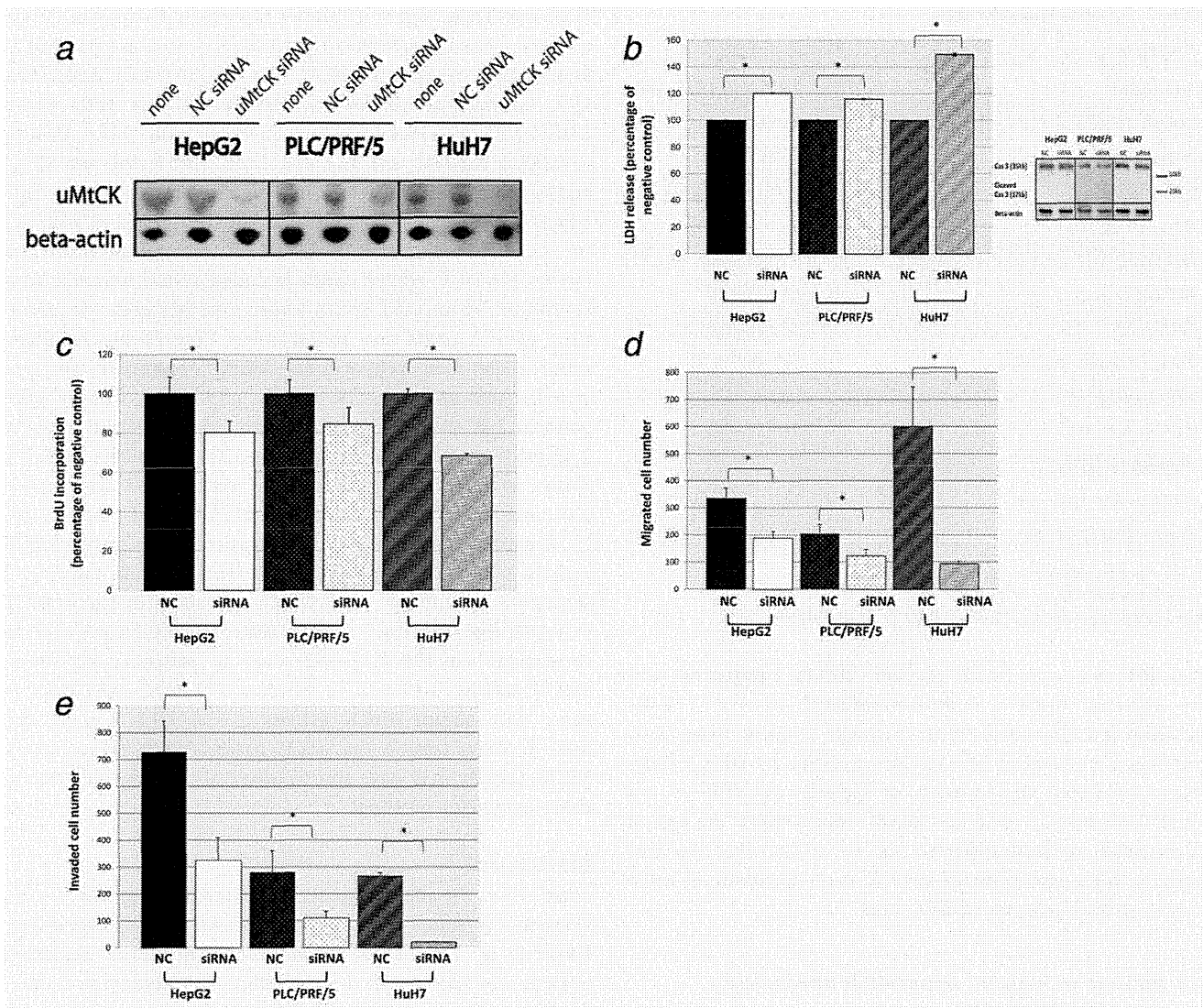


**Figure 3.** Increase in cell death and reduction in proliferation, migration and invasion by reduced uMtCK expression with siRNA in HCC cell lines. Human HCC cell lines, HepG2, PLC/PRF/5 and HuH7 cells, were transfected with 20 nM uMtCK siRNA or universal negative control, and uMtCK levels were examined by immunoblot analysis. None, no transfection; NC, negative control (a). Cell death (b), proliferation (c), migration (d) and invasion (e) were assessed in these HCC cell lines treated with or without uMtCK siRNA. An asterisk indicates a significant difference;  $p < 0.001$  for cell death and proliferation,  $p < 0.02$  for cell migration and invasion from NC.

dehydrogenase released into the culture medium in universal negative control- and uMtCK siRNA-transfected cells (Fig. 3b). In all three cells, transfection with uMtCK siRNA led to an increase in the rate of cell lysis by 20.3% in HepG2, by 15.9% in PLC/PRF/5 and by 49.2% in HuH7, compared to respective control cells transfected with universal negative control ( $p < 0.001$ ). However, caspase 3 activity was not altered in uMtCK siRNA-transfected cells compared to universal negative control-transfected cells (Fig. 3b), suggesting that lactate dehydrogenase release may be explained by some non-specific cell lysis but not by programmed cell death.

Next, to examine a potential association of the reduction in uMtCK expression with cell proliferation rate, BrdU incorporation assay was performed (Fig. 3c). A reduction in cell

proliferation was detected in all three HCC cell lines by 19.8% in HepG2, by 15.5% in PLC/PRF/5 and by 31.7% in HuH7, compared to respective control cells transfected with universal negative control ( $p < 0.001$ ). These results suggest that high expression of uMtCK may play a role in sustaining active proliferation of HCC cells.

The ability of a cancer cell to undergo migration and invasion allows the cell to change position within the tissues. To spread within the tissues, tumor cells use migration and invasion mechanisms. Thus, we investigated the effects of uMtCK inhibition on HCC cell migration and invasion by conducting assays for Matrigel-coated chamber migration and invasion. As shown in Figure 3d, silencing of uMtCK decreased migration rate by 44.1% in HepG2, by 40.0% in

**Table 1.** Baseline characteristics

Parameter	N = 105
Age (year) <sup>1</sup>	70.7 ± 6.7 (49–84)
Male <sup>2</sup>	63 (60.0)
Hepatitis B/C	8 / 97
MtCK (U/L) <sup>3</sup>	9.71 (5.99–19.44)
Albumin (g/dL) <sup>3</sup>	3.4 (3.1–3.9)
AST (U/L) <sup>3</sup>	55 (35–76)
ALT (U/L) <sup>3</sup>	45 (26–60)
GGT (U/L) <sup>3</sup>	37 (28–62)
Total bilirubin (mg/dL) <sup>3</sup>	0.9 (0.7–1.3)
AFP (ng/dL) <sup>3</sup>	18 (8–66)
DCP (mAU/mL) <sup>3</sup>	26 (17–58)
Platelet (×10 <sup>4</sup> /μL) <sup>3</sup>	9.3 (6.3–11.7)
Prothrombin time (sec) <sup>3</sup>	12.1 (11.5–13.1)
Liver stiffness (kPa) <sup>3</sup>	26.3 (18.8–42.2)

<sup>1</sup>Data were expressed as mean ± SD (range).

<sup>2</sup>Data were expressed as number (%).

<sup>3</sup>Data were expressed as median (first to third quartile).

PLC/PRF/5 and by 84.1% in HuH7 cells in comparison with the universal negative control-transfected cells ( $p < 0.02$ ). Furthermore, the results from Matrigel invasion assay indicate that the reduction of uMtCK expression by siRNA transfection inhibited the invasion of HepG2, PLC/PRF/5 and HuH7 cells by 51.7, 62.6 and 92.4%, compared to the universal negative control-transfected cells ( $p < 0.02$ ) (Fig. 3e). Collectively, high expression of uMtCK may contribute to active migration and invasion of HCC cells.

#### HCC patients with higher serum MtCK activity had a poorer prognosis after RFA

Because above *in vitro* results using HCC cell lines suggest that HCC cells with higher expression of uMtCK may have more malignant potential, we next examined a potential association between serum MtCK activity and prognosis in patients with HCC. As described earlier, among two tissue-specific isozymes of MtCK, that is, uMtCK and sarcomeric MtCK, the increase in serum MtCK activity in HCC patients was mostly due to that in serum uMtCK activity but not in serum sarcomeric MtCK activity.<sup>16</sup> To this end, a prognosis of HCC patients, who had been previously enrolled to examine their serum MtCK activity and successfully treated by RFA without residual HCC after the treatment, was analyzed. Characteristics of these 105 HCC patients are shown in Table 1. During the mean follow-up period of 848 days, HCC-related death was observed in 17 patients. First, to evaluate the potential ability of MtCK values to predict survivals or death, a receiver operating characteristic (ROC) curve was generated. The ROC curve showed that a MtCK cutoff of 19.4 U/L had a sensitivity of 76.9% and a specificity of 83.8% for discriminating survivors and deceased patients

(Fig. 4a). Then, Figure 4b shows the actuarial survival curves of these patients subdivided according to their serum MtCK activity prior to RFA for HCC, that is, ≤19.4 U/L and >19.4 U/L; overall survival was shorter in patients with serum MtCK activity >19.4 U/L than in those with ≤19.4 U/L ( $p = 0.0002$ ; log-rank test; Fig. 4b). Then, risk factors for HCC-related death were analyzed. On the univariate analysis, high serum MtCK activity (>19.4 U/L) was a significant risk factor for HCC-related death (Table 2). Other significant risk factors for HCC-related death included serum albumin concentration, serum AST levels, serum total bilirubin concentration, platelet count and prothrombin time (Table 2). Then, multivariate Cox proportional hazard regression analysis revealed that serum MtCK activity >19.4 U/L was an independent risk for HCC-related death, with a hazard ratio of 2.32 (95% confidence interval: 1.03–5.25;  $p = 0.042$ ; Table 2). Serum albumin concentration and serum AST levels were also independently associated with HCC-related death (Table 2). Regarding recurrence, HCC in patients with serum MtCK activity >19.4 U/L recurred earlier than HCC in those with serum MtCK activity ≤19.4 U/L, as depicted in Figure 4c ( $p = 0.004$ ; log-rank test); median (interquartile range) time to recurrence was 189 (107–292) days in patients with serum MtCK activity >19.4 U/L, whereas 278 (160–445) days in those with serum MtCK activity ≤19.4 U/L. Collectively, these findings suggest that HCC patients with higher serum MtCK activity may have shorter survival time possibly due to more malignant potential.

#### Discussion

Little is known about whether there might be an association between the status of mitochondria and uMtCK expression. Kwon *et al.* have reported that ASB9 negatively regulated uMtCK expression with the inhibition of mitochondrial function,<sup>26</sup> suggesting that low uMtCK expression could be associated with loss of mitochondrial integrity. There could be several possibilities regarding the status of mitochondria and uMtCK expression in the liver or HCC; one is that loss of mitochondrial integrity might be associated with reduced uMtCK expression as previously reported.<sup>26</sup> As another possibility, uMtCK expression might be increased as a compensatory mechanism with loss of mitochondrial integrity. In fact, this is exactly the case with sarcomeric MtCK in mitochondrial myopathies.<sup>36</sup> It is also possible that there might be no association in general between loss of mitochondrial integrity and uMtCK expression. In this context, we wondered whether loss of mitochondrial integrity in the liver might be involved in the mechanism of increased uMtCK expression in HCC. To examine this, HCV core gene transgenic mice were used, because these mice develop HCC with loss of mitochondrial integrity in the liver in the absence of inflammation and fibrosis.<sup>22,23</sup> As a result, uMtCK expression was essentially not altered in non-tumorous liver tissues with loss of mitochondrial integrity but clearly enhanced in HCC tissues, suggesting that hepatocarcinogenesis *per se* but not

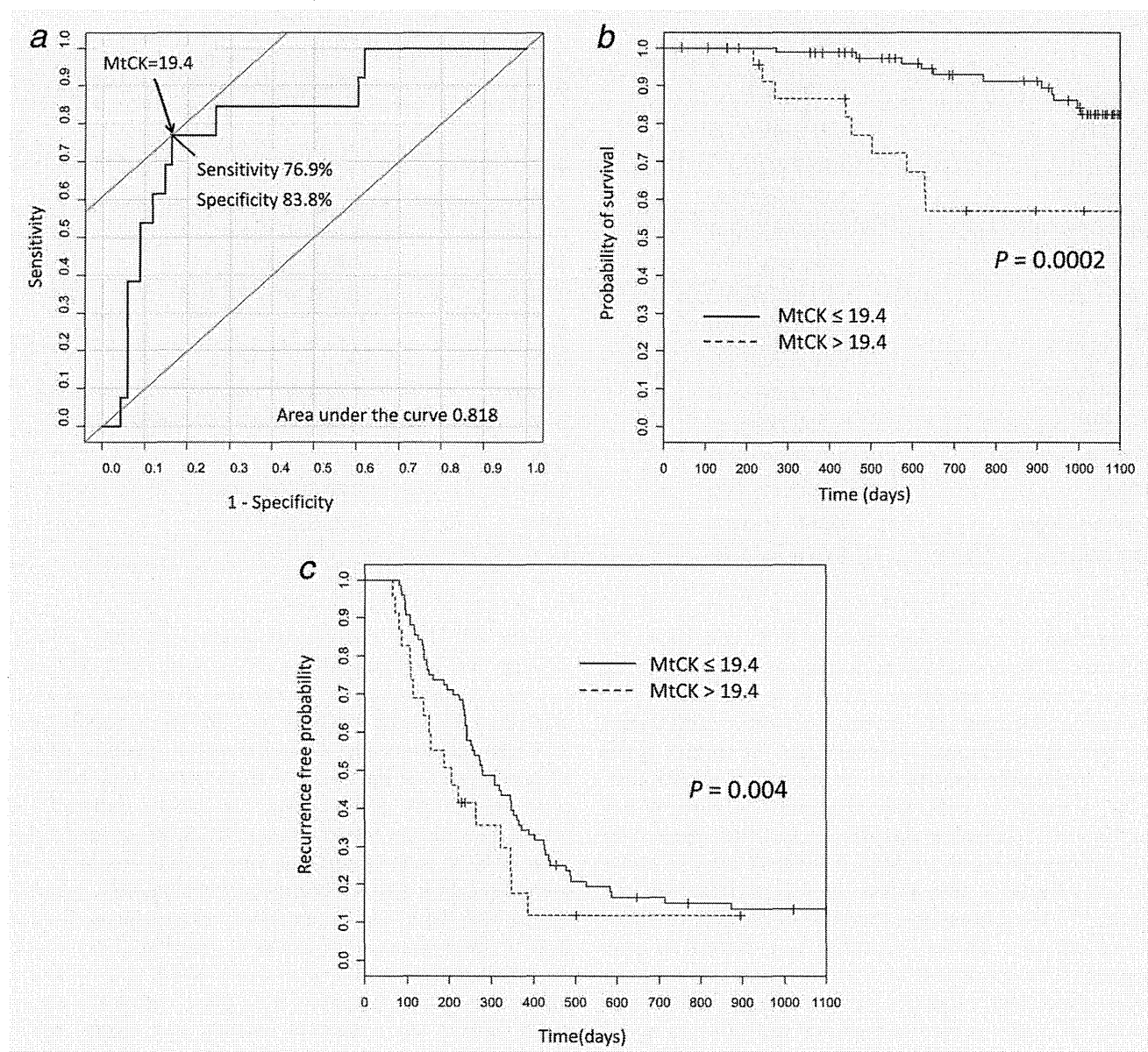


**Figure 4.** (a) ROC curve showing the overall accuracy of serum MtCK activity for discriminating between survivors and deceased patients. The arrow identifies the best cutoff value (i.e., 19.4 U/L) of serum MtCK activity. Kaplan–Meier survival (b) and recurrence (c) curve of the studied patients subdivided according to their serum MtCK activity prior to RFA for HCC. Solid line,  $\leq 19.4$  U/L; dashed line,  $> 19.4$  U/L.

loss of mitochondrial integrity may contribute to increased uMtCK expression in HCC.

Regarding the regulatory mechanism(s) of increased uMtCK expression in HCC, we have found that ASB9 interacted with uMtCK to reduce its protein levels in HCC cells, similarly to HEK293 cells as previously described.<sup>26</sup> In normal liver, uMtCK levels are generally at a very low level, while sarcomeric MtCK as a muscle-specific isoform is not expressed at all,<sup>37</sup> whereas ASB9 mRNA expression is reportedly abundant.<sup>26</sup> Thus, ASB9 may play a physiological role to keep uMtCK protein levels low in the liver. Regarding HCC, ASB9 mRNA expression in HCC cells were much lower than that in normal liver tissue in the current study. This finding

raises the possibility that low expression of ASB9 may explain, at least in part, high protein levels of uMtCK in HCC. Collectively, we may suggest that the two possible mechanisms of increased uMtCK protein levels in HCC cells should be increased gene expression and decreased protein degradation due to reduced ASB9 expression. It has been reported that colorectal cancer with low ASB9 expression may have a higher malignant potential and a poorer prognosis than that with high ASB9 expression,<sup>27</sup> suggesting a negative association of ASB9 with uMtCK protein levels also in colorectal cancer cells. Nonetheless, a potential role of ASB9 in the regulation of uMtCK expression in HCC *in vivo* should be further elucidated.

**Table 2.** Risk factors for HCC-related death evaluated by univariate/multivariate Cox proportional hazard regression

Parameter	Univariate		Multivariate	
	HR (95% CI)	p value	HR (95% CI)	p value
Age (year)	1.02 (0.95–1.10)	0.60		
Female	1.45 (0.56–3.77)	0.44		
Hepatitis B	1.37 (0.18–10.3)	0.76		
MtCK >19.4 (U/L)	5.03 (1.93–13.1)	<0.001	2.32 (1.03–5.25)	0.042
Albumin	0.15 (0.05–0.44)	<0.001	0.26 (0.09–0.71)	0.009
AST	1.02 (1.01–1.03)	<0.001	1.01 (1.00–1.02)	0.028
ALT	1.01 (0.99–1.02)	0.13		
GGT	1.00 (0.98–1.01)	0.45		
Total bilirubin	3.23 (1.98–5.29)	<0.001	1.72 (0.97–3.04)	0.064
AFP >100 (ng/dL)	2.28 (0.84–6.18)	0.11		
DCP >80 (mAU/mL)	2.74 (0.99–7.45)	0.59		
Platelet	0.83 (0.71–0.97)	0.017	0.89 (0.76–1.04)	0.14
Prothrombin time	1.32 (1.11–1.57)	0.002	0.91 (0.70–1.17)	0.45
Liver stiffness	1.02 (0.98–1.04)	0.25		

Reduction of uMtCK expression in HCC cells led to the inhibition in their proliferation, migration and invasion. The similar effects of inhibition of uMtCK expression were reported in Hela cells<sup>29</sup> and breast cancer cells.<sup>17</sup> This finding may be in agreement with the notion that the creatine kinase system is generally essential for the control of cellular energetics in tissues or cells with high and fluctuating energy requirements.<sup>37</sup> Indeed, overexpression has been reported for different creatine kinase isoforms in different types of cancer and has provided a more general growth advantage to solid tumors.<sup>37,38</sup> Overexpression of uMtCK in different Hodgkin-derived cell lines has been described as a marker for poor prognosis.<sup>39</sup> Increased uMtCK levels in cancer cells might be a part of metabolic adaptation of those cells to perform high growth rate under oxygen and glucose restriction as typical for many cancers; it could help to sustain energy turnover, but would be also protective against stress situations such as hypoxia and possibly protect cells from death.<sup>40</sup> Nonetheless, these *in vitro* findings raise the possibility that high expression of uMtCK in HCC may be associated with its active growth and metastasis.

Then, we performed a follow-up study of the HCC patients, with whom we showed the increased serum MtCK activity.<sup>16</sup> Among the entire HCC patients in the previous study, we enrolled the patients who underwent RFA with curative intent to examine the potential association between serum MtCK activity and prognosis in this study. In the previous report, serum MtCK activity was also enhanced in the

patients with liver cirrhosis compared to healthy control, although less prominent than in those with HCC and liver cirrhosis,<sup>16</sup> suggesting that background liver status of HCC may also affect serum MtCK activity. In this context, because RFA with curative intent was performed on patients without advanced liver damages such as high serum total bilirubin concentration, low platelet counts or massive ascites,<sup>33</sup> the potential association between serum MtCK activity and prognosis of HCC patients could be assessed with less bias from background liver status. Furthermore, of note, HCC patients treated with RFA had no extended tumor lesions, that is, three or fewer lesions, each 3.0 cm in diameter.<sup>33</sup> As a result, the HCC patients with higher serum MtCK activity had a significantly poorer prognosis than those with lower serum MtCK activity on a survival analysis, and higher serum MtCK activity was retained as a significant risk for HCC-related death on multivariate analysis. Thus, in line with the current *in vitro* findings, it is suggested that HCC with increased uMtCK expression may have highly malignant potential.

In conclusion, high uMtCK expression in HCC may be caused by hepatocarcinogenesis *per se* but not by loss of mitochondrial integrity, and associated with highly malignant potential, where ASB9 could be one of the regulators of uMtCK expression. In the clinical setting, higher serum MtCK activity was associated with a poorer prognosis of HCC, suggesting that HCC with high serum MtCK activity should be thoroughly treated when considered to be curative.

## References

1. Umemura T, Ichijo T, Yoshizawa K, et al. Epidemiology of hepatocellular carcinoma in Japan. *J Gastroenterol* 2009;44 Suppl 19:102–7.
2. Ferlay J, Shin HR, Bray F, et al. Estimates of worldwide burden of cancer in 2008: GLOBOCAN 2008. *Int J Cancer* 2010;127:2893–917.
3. Bosch FX, Ribes J, Cleries R, et al. Epidemiology of hepatocellular carcinoma. *Clin Liver Dis* 2005; 9:191–211.



4. El-Serag HB, Rudolph KL. Hepatocellular carcinoma: epidemiology and molecular carcinogenesis. *Gastroenterology* 2007;132:2557-76.
5. Baffy G, Brunt EM, Caldwell SH. Hepatocellular carcinoma in non-alcoholic fatty liver disease: an emerging menace. *J Hepatol* 2012;56:1384-91.
6. El-Serag HB, Mason AC. Rising incidence of hepatocellular carcinoma in the United States. *N Engl J Med* 1999;340:745-50.
7. Nakakura EK, Choti MA. Management of hepatocellular carcinoma. *Oncology (Williston Park)* 2000;14:1085-98; discussion 98-102.
8. Davila JA, Kramer JR, Duan Z, et al. Referral and receipt of treatment for hepatocellular carcinoma in United States veterans: effect of patient and nonpatient factors. *Hepatology* 2013;57:1858-68.
9. El-Serag HB, Marrero JA, Rudolph L, et al. Diagnosis and treatment of hepatocellular carcinoma. *Gastroenterology* 2008;134:1752-63.
10. Llovet JM, Ricci S, Mazzaferro V, et al. Sorafenib in advanced hepatocellular carcinoma. *N Engl J Med* 2008;359:378-90.
11. Bertino G, Ardiri A, Malaguarnera M, et al. Hepatocellular carcinoma serum markers. *Semin Oncol* 2012;39:410-33.
12. Bertino G, Ardiri AM, Boemi PM, et al. A study about mechanisms of des-gamma-carboxy prothrombin's production in hepatocellular carcinoma. *Panminerva Med* 2008;50:221-6.
13. Bertino G, Neri S, Bruno CM, et al. Diagnostic and prognostic value of alpha-fetoprotein, des-gamma-carboxy prothrombin and squamous cell carcinoma antigen immunoglobulin M complexes in hepatocellular carcinoma. *Minerva Med* 2011;102:363-71.
14. Bertino G, Ardiri AM, Calvagno GS, et al. Prognostic and diagnostic value of des-gamma-carboxy prothrombin in liver cancer. *Drug News Perspect* 2010;23:498-508.
15. Malaguarnera G, Paladina I, Giordano M, et al. Serum markers of intrahepatic cholangiocarcinoma. *Dis Markers* 2013;34:219-28.
16. Soroida Y, Ohkawa R, Nakagawa H, et al. Increased activity of serum mitochondrial isoenzyme of creatine kinase in hepatocellular carcinoma patients predominantly with recurrence. *J Hepatol* 2012;57:330-6.
17. Qian XL, Li YQ, Gu F, et al. Overexpression of ubiquitous mitochondrial creatine kinase (uMtCK) accelerates tumor growth by inhibiting apoptosis of breast cancer cells and is associated with a poor prognosis in breast cancer patients. *Biochem Biophys Res Commun* 2012;427:60-6.
18. Kanemitsu F, Kawanishi I, Mizushima J, et al. Mitochondrial creatine kinase as a tumor-associated marker. *Clin Chim Acta* 1984;138:175-83.
19. Pratt R, Vallis LM, Lim CW, et al. Mitochondrial creatine kinase in cancer patients. *Pathology* 1987;19:162-5.
20. Onda T, Uzawa K, Endo Y, et al. Ubiquitous mitochondrial creatine kinase downregulated in oral squamous cell carcinoma. *Br J Cancer* 2006;94:698-709.
21. Patra S, Bera S, SinhaRoy S, et al. Progressive decrease of phosphocreatine, creatine and creatine kinase in skeletal muscle upon transformation to sarcoma. *FEBS J* 2008;275:3236-47.
22. Moriya K, Fujie H, Shintani Y, et al. The core protein of hepatitis C virus induces hepatocellular carcinoma in transgenic mice. *Nat Med* 1998;4:1065-7.
23. Moriya K, Nakagawa K, Santa T, et al. Oxidative stress in the absence of inflammation in a mouse model for hepatitis C virus-associated hepatocarcinogenesis. *Cancer Res* 2001;61:4365-70.
24. Kile BT, Schulman BA, Alexander WS, et al. The SOCS box: a tale of destruction and degradation. *Trends Biochem Sci* 2002;27:235-41.
25. Debrincat MA, Zhang JG, Willson TA, et al. Ankyrin repeat and suppressors of cytokine signaling box protein asb-9 targets creatine kinase B for degradation. *J Biol Chem* 2007;282:4728-37.
26. Kwon S, Kim D, Rhee JW, et al. ASB9 interacts with ubiquitous mitochondrial creatine kinase and inhibits mitochondrial function. *BMC Biol* 2010;8:23.
27. Tokuoka M, Miyoshi N, Hitora T, et al. Clinical significance of ASB9 in human colorectal cancer. *Int J Oncol* 2010;37:1105-11.
28. Ikeda H, Nagashima K, Yanase M, et al. Involvement of Rho/Rho kinase pathway in regulation of apoptosis in rat hepatic stellate cells. *Am J Physiol Gastrointest Liver Physiol* 2003;285:G880-6.
29. Lenz H, Schmidt M, Welge V, et al. Inhibition of cytosolic and mitochondrial creatine kinase by siRNA in HaCaT- and HeLaS3-cells affects cell viability and mitochondrial morphology. *Mol Cell Biochem* 2007;306:153-62.
30. Makuuchi M, Kokudo N, Arai S, et al. Development of evidence-based clinical guidelines for the diagnosis and treatment of hepatocellular carcinoma in Japan. *Hepatol Res* 2008;38:37-51.
31. Torzilli G, Minagawa M, Takayama T, et al. Accurate preoperative evaluation of liver mass lesions without fine-needle biopsy. *Hepatology* 1999;30:889-93.
32. Hoshino T, Sakai Y, Yamashita K, et al. Development and performance of an enzyme immunoassay to detect creatine kinase isoenzyme MB activity using anti-mitochondrial creatine kinase monoclonal antibodies. *Scand J Clin Lab Invest* 2009;69:687-95.
33. Omata M, Tateishi R, Yoshida H, et al. Treatment of hepatocellular carcinoma by percutaneous tumor ablation methods: ethanol injection therapy and radiofrequency ablation. *Gastroenterology* 2004;127:S159-66.
34. Nishikawa M, Nishiguchi S, Shiomi S, et al. Somatic mutation of mitochondrial DNA in cancerous and noncancerous liver tissue in individuals with hepatocellular carcinoma. *Cancer Res* 2001;61:1843-5.
35. Tamori A, Nishiguchi S, Nishikawa M, et al. Correlation between clinical characteristics and mitochondrial D-loop DNA mutations in hepatocellular carcinoma. *J Gastroenterol* 2004;39:1063-8.
36. Stadhouders AM, Jap PH, Winkler HP, et al. Mitochondrial creatine kinase: a major constituent of pathological inclusions seen in mitochondrial myopathies. *Proc Natl Acad Sci USA* 1994;91:5089-93.
37. Schlattner U, Tokarska-Schlattner M, Wallimann T. Mitochondrial creatine kinase in human health and disease. *Biochim Biophys Acta* 2006;1762:164-80.
38. Wyss M, Kaddurah-Daouk R. Creatine and creatinine metabolism. *Physiol Rev* 2000;80:1107-213.
39. Kornacker M, Schlattner U, Wallimann T, et al. Hodgkin disease-derived cell lines expressing ubiquitous mitochondrial creatine kinase show growth inhibition by cyclocreatine treatment independent of apoptosis. *Int J Cancer* 2001;94:513-9.
40. Dang CV, Semenza GL. Oncogenic alterations of metabolism. *Trends Biochem Sci* 1999;24:68-72.

**Original Article**

# Potential associations between perihepatic lymph node enlargement and liver fibrosis, hepatocellular injury or hepatocarcinogenesis in chronic hepatitis B virus infection

Masaya Sato,<sup>1,2</sup> Hiromi Hikita,<sup>1</sup> Shu Hagiwara,<sup>1</sup> Mamiko Sato,<sup>1</sup> Yoko Soroida,<sup>1</sup> Atsushi Suzuki,<sup>1</sup> Hiroaki Gotoh,<sup>1</sup> Tomomi Iwai,<sup>1</sup> Soichi Kojima,<sup>3</sup> Tomokazu Matsuura,<sup>4</sup> Hiroshi Yotsuyanagi,<sup>5</sup> Kazuhiko Koike,<sup>2</sup> Yutaka Yatomi<sup>1</sup> and Hitoshi Ikeda<sup>1</sup>

Departments of <sup>1</sup>Clinical Laboratory Medicine, <sup>2</sup>Gastroenterology and <sup>5</sup>Infectious Disease, Graduate School of Medicine, The University of Tokyo, <sup>4</sup>Department of Laboratory Medicine, The Jikei University School of Medicine, Tokyo, and <sup>3</sup>Regulation Technology Unit, RIKEN Center for Life Science Technologies, Wako, Saitama, Japan

**Aim:** Although perihepatic lymph node enlargement (PLNE) is frequently observed in chronic liver disease, little is known about PLNE in chronic hepatitis B virus (HBV) infection. We aimed to evaluate this issue.

**Methods:** We originally enrolled a consecutive 502 patients with chronic HBV infection. Among them, 288 patients without history of interferon-based or nucleoside analog treatment and hepatocellular carcinoma (HCC) were primarily analyzed.

**Results:** PLNE was detected in 27 of 288 (9.4%) patients, which was fewer than that in chronic hepatitis C patients but more than that in subjects undertaking a general health examination as previously reported. The presence of PLNE was significantly associated with a higher probability of having an aspartate aminotransferase (AST) platelet ratio

index of more than 1.5 (11.1% vs 1.5%,  $P = 0.01$ ), a higher AST level (38.0 vs 26.8 U/L,  $P = 0.001$ ), a higher alanine aminotransferase level (50.1 vs 28.0 U/L,  $P < 0.0001$ ), and a lower platelet count ( $18.6$  vs  $20.6 \times 10^4/\mu\text{L}$ ,  $P = 0.048$ ) after adjustment for sex and age. However, in our original sample ( $n = 502$ ), PLNE was observed in 1.4% of the patients with HCC and/or its history whereas 9.2% of the patients without HCC, and the proportion was significantly lower in patients with HCC and/or its history ( $P = 0.03$ ).

**Conclusion:** PLNE was associated with liver fibrosis and hepatocellular injury, but was negatively associated with HCC in chronic HBV infection.

**Key words:** fibrosis, hepatitis B, immune response, inflammatory activity, perihepatic lymph node enlargement

## INTRODUCTION

HEPATITIS B VIRUS (HBV) infection is an important cause of chronic liver disease globally, with an estimated 350 million carriers worldwide.<sup>1</sup> Chronic HBV infection is a major risk factor for several liver diseases, such as chronic hepatitis B (CHB), liver cirrhosis and hepatocellular carcinoma (HCC),<sup>2</sup> which is the

fifth most common cancer worldwide.<sup>3</sup> HBV infection itself is non-cytopathic, and it is the immune response to the viral antigens that are thought to be responsible for the necroinflammatory process involved in chronic infection, cirrhosis and HCC.<sup>4</sup>

Perihepatic lymph node enlargement (PLNE) is frequently observed in patients with chronic liver disease,<sup>5</sup> especially in those with hepatitis C virus (HCV) infection.<sup>6,7</sup> Although some studies have reported that PLNE was associated with inflammatory activity, stage of liver fibrosis or hepatitis viral load,<sup>7-12</sup> such associations were inconsistent among other studies,<sup>6-8,10-15</sup> suggesting that the clinical significance of PLNE in HCV infection has not been fully established yet. We have recently reported that PLNE is negatively associated with the response to interferon (IFN)-based treatment or development of HCC in patients with chronic hepatitis C (CHC).<sup>16,17</sup> It is

Correspondence: Dr Hitoshi Ikeda, Department of Clinical Laboratory Medicine, Graduate School of Medicine, The University of Tokyo, 7-3-1 Hongo, Bunkyo-ku, Tokyo 113-8655, Japan. Email: ikeda-1im@h.u-tokyo.ac.jp

Conflict of interest: None of the authors have any conflicts of interest.

Received 11 November 2013; revision 3 April 2014; accepted 15 May 2014.

reported that PLNE is a relatively common finding in patients with primary biliary cirrhosis among other liver diseases.<sup>15</sup>

On the other hand, the reports regarding PLNE in patients with chronic HBV infection have been scarce. The purpose of the present study was to evaluate the clinical significance of PLNE in chronic HBV infection.

## METHODS

### Patients and screening for PLNE

WE ENROLLED 502 consecutive patients with chronic HBV infection who underwent ultrasonography (US) between November 2012 and April 2013 at the Department of Clinical Laboratory, the University of Tokyo Hospital. Patients with chronic HBV infection were defined as those positive for hepatitis B surface antigen for at least 6 months. Patients who were positive for HCV RNA and had a history of other hepatobiliary disease were excluded. All patients took laboratory blood tests at the time they underwent US. Aspartate aminotransferase (AST) platelet ratio index (APRI) was used to assess liver fibrosis, and APRI of more than 1.5 was classified as bridging fibrosis or cirrhosis (F stage 3–4).<sup>18</sup> The criteria to identify PLNE were previously described; PLNE was defined as a lymph node at the perihepatic area measuring 1 cm or more in the longest axis.<sup>17</sup> In the analysis to examine the association between PLNE and clinical findings, we excluded the patients receiving IFN or nucleoside analog treatment, or having HCC or a history of HCC from the primary analysis.

The present study was carried out in accordance with the ethical guidelines of the Declaration of Helsinki and was approved by the Institutional Research Ethics Committees of the authors' institutions.

### Study end-points

We examined the association between PLNE and clinical findings such as liver fibrosis, hepatocellular injury or the presence of HCC in patients with chronic HBV infection (the primary end-point of this study). We previously reported the prevalence of PLNE in the patients with CHC<sup>17</sup> or the patients underwent general health examinations (general population).<sup>19</sup> Using the results of our previous studies, we then compared the prevalence of PLNE in the patients with chronic HBV infection to patients with CHC or general population (the secondary end-point).

## Statistical analysis

Continuous variables were presented as the mean  $\pm$  standard deviation (SD), while categorical variables were expressed as frequencies (%). Categorical data were analyzed using the  $\chi^2$ -test or Fisher's exact test, and stepwise logistic regression model analyses were used to adjust the contribution of PLNE by other covariates such as sex or age. For continuous data, the univariate associations were evaluated using Student's *t*-test. Stepwise regression model analyses were used to adjust the contribution of PLNE by other covariates such as sex or age. The Cochran–Armitage trend test was used for assessing increasing or decreasing trends in binomial proportions. All statistical analyses were two-sided, and the threshold of the reported *P*-values for significance was accepted as less than 0.05. All statistical analyses were performed using R statistic software version 2.15.2 (<http://www.r-project.org>).

## RESULTS

### Patient characteristics and association between PLNE and clinical findings

TO EXAMINE THE association between PLNE and clinical findings, patients receiving IFN or nucleoside analog treatment, and those with HCC or past history of HCC were excluded from the primary analysis, because antiviral treatment or HCC could directly influence PLNE. As a result, the data of 288 among 502 patients were primarily analyzed. Characteristics of these patients are shown in Table 1. Overall, 51.0% (147) were male, and the mean age was 53.72 years. PLNE were detected in 27 of 288 (9.4%) patients, and the mean length of the longest axis was 1.6 cm (range, 1.0–3.2).

Table 2 shows the relationships between PLNE and various clinical findings. The presence of PLNE was significantly associated with a higher APRI value of more than 1.5 ( $P=0.01$ ), a higher serum AST level ( $P=0.001$ ), a higher serum alanine aminotransferase (ALT) level ( $P<0.0001$ ), and a lower platelet count ( $P=0.048$ ) after adjustment for sex and age, suggesting that PLNE may be observed in patients with more liver fibrosis and more hepatocellular injury. We also compared the correlation between PLNE and clinically diagnosed liver cirrhosis. Diagnosis of cirrhosis is based on the presence of clinical and laboratory features of portal hypertension (the presence of esophageal varices and/or collateral circulation at endoscopy and ultrasound) and/or liver stiffness measurement value more than

**Table 1** Patient characteristics ( $n = 288$ )

Parameter	Values
Mean age (years)	53.72 ± 14.74
Sex	
Male	147 (51.0%)
Female	141 (49.0%)
PLNE	
Present	27 (9.4%)
Absent	261 (90.6%)
Perihepatic lymph node diameter†	1.6 (1.0–3.2)‡
APRI score	
>1.5	7 (2.4%)
≤1.5	281 (97.6%)
Mean HBV DNA (log <sup>10</sup> copies/mL)	3.97 ± 2.13
Mean AST (U/L)	27.83 ± 17.37
Mean ALT (U/L)	30.09 ± 30.68
Mean TB (mg/dL)	0.93 ± 0.57
Mean albumin (g/dL)	4.20 ± 0.34
Mean platelet count (×10 <sup>4</sup> /μL)	20.43 ± 6.01
Mean γ-GT (U/L)	39.26 ± 108.55
Mean PT-INR	0.95 ± 0.14

†In PLNE positive patients.

‡Median (range).

Continuous variables are represented as the mean ± standard deviation and categorical variables were as number and frequencies (%).

γ-GT, γ-glutamyltransferase; ALT, alanine aminotransferase; APRI, aspartate aminotransferase-to-platelet ratio index; AST, aspartate aminotransferase; HBV, hepatitis B virus; PLNE, perihepatic lymph node enlargement; PT-INR, prothrombin time international normalized ratio; TB, total bilirubin.

16.9 kPa which was reported to be the optimal diagnostic accuracy.<sup>20</sup> Of the patients, 18.5% (5/27) with PLNE and 2.7% (7/261) without PLNE were clinically diagnosed with liver cirrhosis. The prevalence of the patients with clinically diagnosed liver cirrhosis was significantly higher in the patients with PLNE ( $P = 0.0009$ ) after adjustment for sex and age (data not shown). In addition, there was a trend that serum HBV DNA level was higher in patients with PLNE than in those without, although not statistically significant (Table 2).

We then compared the prevalence of PLNE among asymptomatic carrier (APRI, ≤1.5; ALT, ≤30), patients with chronic hepatitis (APRI, ≤1.5; ALT, >30) and patients with cirrhosis (APRI, >1.5). PLNE was detected in 8.3% (17/206) of asymptomatic carriers, 9.3% (7/75) of patients with chronic hepatitis and 42.9% (3/7) of patients with cirrhosis (Fig. 1). The progression of liver disease was significantly associated with higher prevalence of PLNE ( $P = 0.03$ ), as demonstrated by the

Cochran–Armitage trend test. We also examined the association between hepatitis B e (HBe) status and the prevalence of PLNE. PLNE was detected in 18.8% (6/32) of the patients positive for HBe antigen (HBeAg) and 8.3% (21/251) of the patients negative for HBeAg. Prevalence of PLNE was higher in the patients with positive for HBeAg, however, the difference did not reach statistical significance ( $P = 0.11$ ).

### Comparison of the frequency of PLNE in patients with HCC and/or its history and those without HCC

Because our current findings suggest the associations between PLNE and liver fibrosis, hepatocellular injury or serum HBV DNA level in patients with chronic HBV infection, we wondered whether PLNE might be observed more frequently in those with HCC and/or its past history than in those without. On the other hand, PLNE was reportedly a negative risk for hepatocarcinogenesis in CHC patients. Thus, these results prompted us to examine how PLNE could be associated with HCC in patients with chronic HBV infection.

To address this question, we compared the frequency of PLNE in patients with HCC and/or its history and in those without in our original sample ( $n = 502$ ). Table 3 shows the patient characteristics and the associations between prevalence of HCC and clinical findings. PLNE was detected in 1.4% (1/69) of the patients with HCC and/or its history and 9.2% (40/433) of the patients without HCC, where the patients receiving IFN or nucleoside analog treatment were also included in the analysis. As shown in Figure 2 and Table 3, the frequency of PLNE was significantly lower in patients with HCC and/or its history than in those without ( $P = 0.03$ ). Then, we tested PLNE and the following variables on multivariate analysis: age, sex, APRI score, ALT, total bilirubin, albumin and γ-glutamyltransferase. As a result, the association between PLNE and lower probability of HCC was noted, although not statistically significant ( $P = 0.057$ ). In this multivariate analysis, higher prevalence of HCC was significantly associated with older age ( $P = 0.01$ ), male sex ( $P = 0.009$ ), higher APRI score ( $P = 0.0002$ ) and lower ALT level ( $P = 0.0006$ ) (data not shown).

### Comparison of the frequency of PLNE with liver diseases of other etiology

Perihepatic lymph node enlargements were detected in 27 of 288 (9.4%) of the patients without treatment for